Author for correspondence:
Jade E. Hatton
e-mail: j.e.hatton@bristol.ac.uk

THE ROYAL SOCIETY
PUBLISHING

Silicon isotopes in Arctic and sub-Arctic glacial meltwaters: the role of subglacial weathering in the silicon cycle

Jade E. Hatton[1], Katharine R. Hendry[1], Jonathan R. Hawkings[3,4], Jemma L. Wadham[2], Sophie Opfergelt[5], Tyler J. Kohler[6,7], Jacob C. Yde[8], Marek Stibal[6] and Jakub D. Žárský[6]

[1]School of Earth Sciences, and [2]School of Geographical Sciences, University of Bristol, Bristol, UK
[3]National High Magnetic Field Lab and Earth, Ocean and Atmospheric Sciences, Florida State University, Tallahassee, FL, USA
[4]German Research Centre for Geosciences GFZ, Potsdam, Germany
[5]Earth and Life Institute, Environmental Sciences, Université Catholique de Louvain, L7.05.10, 1348, Louvain-la-Neuve, Belgium
[6]Department of Ecology, Faculty of Science, Charles University, Prague, Czechia
[7]Stream Biofilm and Ecosystem Research Laboratory, School of Architecture, Civil and Environmental Engineering, École Polytechnique Fédérale de Lausanne, 1015 Lausanne, Switzerland
[8]Department of Environmental Sciences, Western Norway University of Applied Sciences, Sogndal, Norway

JEH, 0000-0002-9408-7981; KRH, 0000-0002-0790-5895

Glacial environments play an important role in high-latitude marine nutrient cycling, potentially contributing significant fluxes of silicon (Si) to the polar oceans, either as dissolved silicon (DSi) or as dissolvable amorphous silica (ASi). Silicon is a key nutrient in promoting marine primary productivity, contributing to atmospheric CO_2 removal. We present the current understanding of Si cycling in glacial systems, focusing on the Si isotope ($\delta^{30}Si$) composition of glacial meltwaters. We combine existing glacial $\delta^{30}Si$ data with new measurements from 20 sub-Arctic glaciers, showing that glacial meltwaters

consistently export isotopically light DSi compared with non-glacial rivers (+0.16‰ versus +1.38‰). Glacial $\delta^{30}Si_{ASi}$ composition ranges from -0.05‰ to -0.86‰ but exhibits low seasonal variability. Silicon fluxes and $\delta^{30}Si$ composition from glacial systems are not commonly included in global Si budgets and isotopic mass balance calculations at present. We discuss outstanding questions, including the formation mechanism of ASi and the export of glacial nutrients from fjords. Finally, we provide a contextual framework for the recent advances in our understanding of subglacial Si cycling and highlight critical research avenues for assessing potential future changes in these environments.
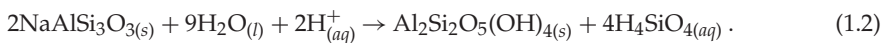
1. Review of active processes within the Si cycle

Physical and chemical weathering in subglacial environments results in the export of key nutrients to the ocean that are required for marine primary production [1–13]. Understanding the silicon (Si) cycle is key to the consideration of the carbon cycle, because of the coupling between the two. Silicon is a vital nutrient for diatoms, siliceous algae, that account for approximately 40% of oceanic carbon export [14–16]. The Si cycle has been well described in recent years [17–21]. Broadly, there are two relatively distinct sub-cycles: continental and oceanic. Initially, dissolved Si (DSi) is liberated from silicate minerals through chemical weathering in the form of H_4SiO_4 [22,23]. The subsequent formation and burial of marine carbonates results in the sequestration of atmospheric CO_2, hence silicate weathering is also an important sink of CO_2 on geological time scales [21]. Equations (1.1)–(1.3) outline examples of the silicate weathering reactions that occur, including those hypothesized under glaciers.
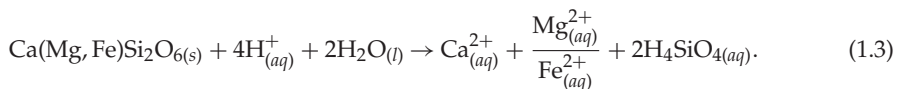
Equation (1.1), weathering of anorthite:

$$\left.\begin{array}{l} CaAl_2Si_2O_{8(s)} + 2CO_{2(aq)} + 8H_2O_{(l)} \rightarrow Ca^{2+}_{(aq)} + 2Al(OH)_{3(s)} + 2H_4SiO_{4(aq)} + 2HCO^-_{3(aq)}, \\ Ca^{2+}_{(aq)} + 2HCO^-_{3(aq)} \rightarrow CaCO_{3(s)} + H_2CO_{3(aq)}. \end{array}\right\} \tag{1.1}$$
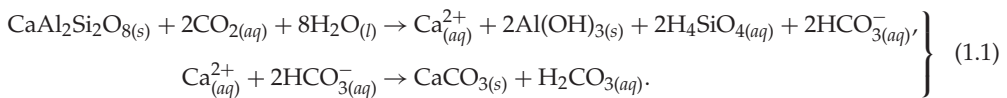
Equation (1.2), silicate hydrolysis of albite:

$$2NaAlSi_3O_{3(s)} + 9H_2O_{(l)} + 2H^+_{(aq)} \rightarrow Al_2Si_2O_5(OH)_{4(s)} + 4H_4SiO_{4(aq)}. \tag{1.2}$$

Equation (1.3), congruent weathering of pyroxene:

$$Ca(Mg, Fe)Si_2O_{6(s)} + 4H^+_{(aq)} + 2H_2O_{(l)} \rightarrow Ca^{2+}_{(aq)} + \frac{Mg^{2+}_{(aq)}}{Fe^{2+}_{(aq)}} + 2H_4SiO_{4(aq)}. \tag{1.3}$$

The resultant DSi is transported to the oceans predominantly via rivers and groundwater [17], and as biogenic phases formed by the secretion of silica (i.e. silicon dioxide) by primary producers, such as diatoms and higher plants. We now have improved budgets of numerous aspects of the Si cycle, which can be used when attempting to estimate input and output fluxes to the ocean [17,18]. Riverine fluxes comprise the main input of Si into the oceans (7.3–8.1 Tmol yr^{-1}, [17,19]), but other inputs also include aeolian dust (0.3 Tmol yr^{-1}), groundwater (0.6 Tmol yr^{-1}) and hydrothermal fluids (0.6 Tmol yr^{-1}) according to Cornelis *et al.* [24] and Frings *et al.* [17]. However, data from glacial environments are still rare, which could have important implications especially when quantifying the riverine inputs to high-latitude oceans.

Glacier melting has accelerated over the past two decades, with Greenland Ice Sheet (GrIS) freshwater fluxes into the Irminger Basin increasing by 50% in less than 20 years [25]. Similarly, overall GrIS discharge has accounted for approximately 1000 km^3 of freshwater discharge into the ocean per year between 2000 and 2010 [26–29], with rapid, nonlinear increases in run-off expected in the future [29]. Increased melting and resultant changes in hydrological pathways and subglacial water sources are likely to have an impact on dissolved nutrient export [1] and long-term climate modulation through the global carbon cycle [30]. Glacial weathering also results

in the production of finely ground glacial flour, meaning a large fraction of nutrients exported in glacial meltwaters are associated with suspended sediments [1,31]. However, the future of suspended sediment fluxes from glacial environments is uncertain [32], and may depend on changes to surface melting, induced ice motion and subglacial hydrological drainage [33,34].

Knowledge of current glacial biogeochemical processes and their drivers within the subglacial environment is crucial to our understanding of how glacial nutrient fluxes and the resultant impact on downstream ecosystems may respond under climatic warming scenarios.

The purposes of this paper are as follows.

(i) Present new DSi and amorphous silica (ASi) data (both concentrations and Si isotopic composition) from a range of Arctic and sub-Arctic glaciers.
(ii) Compare the isotopic composition of Si from glacial meltwaters with that from non-glacial rivers and consider the main hypotheses for the mechanisms driving the differences between the measured values, in the context of subglacial weathering processes.
(iii) Discuss the potential implications of these findings for interpretations of the past global Si cycle, and future scenarios as glacial environments respond to anthropogenic climatic change.

This work builds on reviews of continental Si cycling by Opfergelt & Delmelle [20] and Frings *et al.* [17] by considering the role of glacial systems on terrestrial fluxes of Si into the oceans and glacial weathering influence on Si isotope composition. It will focus on Arctic and sub-Arctic glacial systems, as this is where studies into δ^{30}Si composition of glacial rivers have been conducted so far, and our understanding of the weathering processes and fluxes from these environments is most complete. Unfortunately, there are no δ^{30}Si data from Antarctica and temperate alpine glaciers, preventing this review from conducting a global assessment of δ^{30}Si composition from glacial rivers. However, the combination of new data from 20 Arctic and sub-Arctic glaciers and the existing data with published literature enables a useful consideration of glacial δ^{30}Si composition, and the potential subglacial drivers and impact upon the wider Si cycle.

(a) Silicon isotope fractionation in low-temperature Earth surface processes

Silicon isotopes are a powerful tool for understanding geochemical processes within modern and past environments [17]. Silicon has three stable isotopes, ^{28}Si, ^{29}Si and ^{30}Si, with respective abundances of approximately 92.18%, 4.68% and 3.15% [35]. The Si isotopic composition is reported in delta notation in terms of ^{29}Si or ^{30}Si. Here, we will report data in terms of δ^{30}Si, according to equation (1.4),

$$\delta^{30}\text{Si} = \left[\frac{(^{30}\text{Si}/^{28}\text{Si})\text{sample}}{(^{30}\text{Si}/^{28}\text{Si})\text{NBS28}} - 1 \right] \times 1000. \tag{1.4}$$

Samples are reported against a known reference standard, most commonly NBS28 (RM 8546), which is a quartz standard distributed by the National Institute of Standards and Technology (NIST). Fractionation occurring during Earth surface processes, as a result of both kinetic and equilibrium effects, is mass dependent such that values of δ^{30}Si are related in a predictable manner to δ^{29}Si, δ^{29}Si $\sim 0.5 \times \delta^{30}$Si [17,36]. The fractionation factor is reported as α (equation (1.5)) and is calculated as the fractionation from the substrate (A) to the product (B). Since the numerical value of α_{A-B} is usually very close to 1, it is also expressed in terms of per mil notation (ε, equation (1.6)) [17,18],

$$\alpha_{A-B} = \frac{(^{30}\text{Si} : ^{28}\text{Si})_A}{(^{30}\text{Si} : ^{28}\text{Si})_B} \tag{1.5}$$

and

$$\varepsilon = 1000 \cdot (\alpha_{A-B} - 1). \tag{1.6}$$

Natural processes occurring at the Earth surface often comprise a complex chain of reactions, and quantification of the contribution of each step to the overall stable Si isotope fractionation is challenging. However, observations reveal that there is some common isotopic fractionation behaviour during low-temperature biogeochemical processes. When silicate minerals are weathered, forming secondary weathering products, the newly formed solids will be enriched with the lighter isotopes, compared with the parent rock and the residual waters which will be isotopically heavier [17,37]. Similarly, biological processes also result in the fractionation of Si. The uptake of silicic acid by primary producers, such as plants and diatoms, and/or the conversion of this to biogenic silica (BSi) preferentially incorporates the lighter isotopes into the newly formed BSi, leading to residual waters becoming isotopically heavy [38–40].

The magnitude of fractionation is dependent on numerous environmental factors, with laboratory studies attempting to quantify fractionation factors producing a large range of values. Experiments of ASi precipitation below 50°C by Geilert *et al.* [41] found a range of fractionation factors from +0.1‰ to −2.1‰, with lower temperatures producing the largest fractionation factors. However, they also found that these fractionation factors were influenced by mineral surface area, saturation state and flow regime, making it challenging to apply their findings to the natural environment. In comparison, precipitation experiments by Oelze *et al.* [42] found no fractionation during the formation of almost pure Si solids, but experiments with high Al/Si ratios produced fractionation factors of up to −5‰, with regimes beginning as unidirectional but shifting towards steady state once re-dissolution began. These two laboratory experiments present advances in our understanding of the magnitude of fractionation in low-temperature environments, but also highlight the difficulties in applying laboratory findings to real-world data owing to the complexity of the systems.

Rivers integrate the complex biogeochemical reactions occurring during weathering and biological utilization within their catchments, capturing the overall isotopic fractionation during these low-temperature processes [38,43–46]. The mean isotopic composition of dissolved riverine Si ($\delta^{30}Si_{DSi}$) is currently reported as +1.25‰, from at least 557 individual measurements [17]. The isotopic composition of riverine waters can be linked to chemical weathering processes [47–49], as measurements show that the secondary weathering products are isotopically lighter than the DSi of river waters. Sutton *et al.* [18] conceptualized the processes as a mass balance between 'kinetically limited' and 'supply limited' to show how Si fluxes and isotopic composition are influenced by a balance of weathering and physical erosional processes. Kinetically limited systems are those where there is an excess of fresh material to be weathered but weathering fluxes are limited by external conditions, such as temperature. This best describes a subglacial environment, whereas supply-limited systems are those constrained by the supply of fresh weatherable material and thus almost all of the material is exported from the catchment as a dissolved flux [18].

To date, two key observations have been made when considering the $\delta^{30}Si_{DSi}$ of rivers [17,18]. First, the $\delta^{30}Si_{DSi}$ composition of rivers is almost always higher than the parent material from which it has derived. Second, there is often a pronounced seasonal variation of approximately 0.5–1.0‰, with the lighter compositions linked to times of higher riverine discharge [17]. One important exception exists: the $\delta^{30}Si_{DSi}$ composition of glacial meltwaters within proglacial rivers does not fit the observation that the $\delta^{30}Si_{DSi}$ composition will be higher than the parent material [50]. The benefit of using Si isotopes in glacial systems to trace subglacial weathering processes is the lack of interference from primary productivity within proglacial streams. Proglacial rivers are extremely turbid owing to the high suspended sediment loads, resulting in an unfavourable environment for primary producers such as diatoms. Therefore, the Si isotope composition measured in these environments can be attributed to weathering processes, without the requirement of coupling the measurements with other isotope systems to deconvolve biological effects; e.g. Pogge von Strandmann *et al.* [38]. Understanding the drivers behind isotopic fractionation in subglacial environments may therefore provide insight into subglacial weathering regimes which are inherently different from those driving the $\delta^{30}Si_{DSi}$ composition of non-glacial rivers (as detailed further in §1b, figure 1).
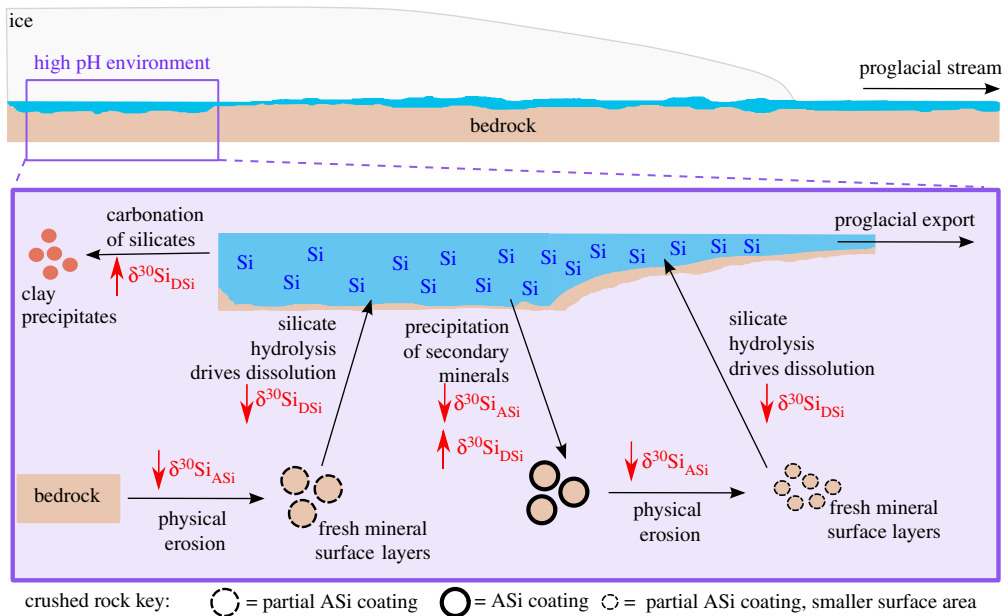
Figure 1. Conceptual model tracing subglacial processes impacting upon dissolved silicon isotope composition ($\delta^{30}Si_{DSi}$) and silicon isotope composition in amorphous silica ($\delta^{30}Si_{ASi}$). The hypothesized change in $\delta^{30}Si$ composition as a result of each subglacial processes is denoted by red arrows. The pH of the environment is high as a result of alkalinity from silicate hydrolysis reactions. (Online version in colour.)
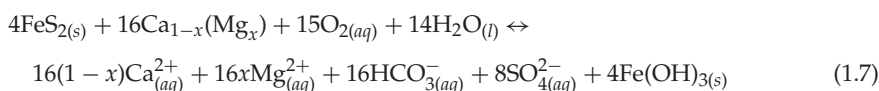
(b) Understanding subglacial weathering processes

In order to predict the fluxes of key nutrients exported from glacial environments in the future we need to understand the mechanisms driving them, especially considering the complex nature of subglacial weathering processes, which are dependent upon subglacial hydrological evolution, bedrock lithology, and microbial community abundance and composition. As a result, hydrochemistry in proglacial rivers is often very different from that in non-glacial rivers, so the proportions of typical riverine weathering reactions cannot necessarily be applied in these environments. For example, initial studies of glacierized catchments, which focused on small glaciers, found glacial meltwaters to be lower in Si than non-glacial rivers [51–53]. More recent compilations of data from various glacierized catchments, including much larger catchments, also showed that dissolved $K^+ : Na^+$ ratios (indicative of silicate mineral dissolution) are higher from glacial environments than data from the world's largest rivers, and ratios of $Ca^{2+} : Na^+$ and $SO_4^{2-} : Na^+$ are also significantly different [54], despite lower Si in glacial rivers. Chemical weathering yields from glacierized catchments (indicated by cation loading) have been shown to be above average when considering global rivers, because of the high run-off and physical erosion from these environments [54]. Conceptual models of the subglacial weathering processes that result in these distinct proglacial river chemistries have also been described previously [55–58].
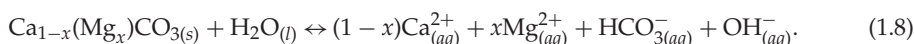
Subglacial environments have complex hydrological systems, which develop seasonally [57,59]. This heterogeneity results in some areas of the bed with isolated waters and inefficient drainage pathways (i.e. tortuous flow paths), and other areas with efficient drainage pathways and short residence time waters [57]. This leads to differences in saturation state of primary and secondary minerals, and varying dissolution/precipitation reactions. Evolution and connection of hydrological flow paths and the introduction of supraglacial water will also impact water residence times and biogeochemical properties [60]. The efficiency of the subglacial pathways changes through an ablation season, which is true of small and large glacial systems [57,61,62], although predicting when changes will occur is difficult because of the complex nature of the

subglacial system and inter-annual variability [63]. Such complex and temporally heterogeneous processes are likely to result in variations in isotopic fractionation in these environments.

Some of the first in-depth geochemical studies of subglacial weathering reactions took place at Haut Glacier d' Arolla in the Swiss Alps [57,64]. Here, the subglacial waters, sampled via boreholes, were split into three categories (Types A, B and C), demonstrating the heterogeneity within the subglacial environments. Type A waters were the most concentrated in major ions, predicted to form in hydrologically inefficient areas. Type B waters were the most common waters, derived from more efficient parts of the drainage system, with chemical composition likely to be influenced by water residence time. Type C waters were the most dilute but had high turbidity, potentially representative of channel marginal zones [57]. Each water type was dominated by distinct geochemical reactions, for example waters in inefficient distributed systems were dominated by coupled sulfide oxidation–carbonate dissolution (equation (1.7)), whereas samples from more efficient pathways had higher DSi, potentially as a result of high pH (due to carbonate or silicate hydrolysis (equations (1.8) and (1.2)) promoting Si dissolution,

$$4FeS_{2(s)} + 16Ca_{1-x}(Mg_x) + 15O_{2(aq)} + 14H_2O_{(l)} \leftrightarrow$$
$$16(1-x)Ca^{2+}_{(aq)} + 16xMg^{2+}_{(aq)} + 16HCO^-_{3(aq)} + 8SO^{2-}_{4(aq)} + 4Fe(OH)_{3(s)} \tag{1.7}$$

and

$$Ca_{1-x}(Mg_x)CO_{3(s)} + H_2O_{(l)} \leftrightarrow (1-x)Ca^{2+}_{(aq)} + xMg^{2+}_{(aq)} + HCO^-_{3(aq)} + OH^-_{(aq)}. \tag{1.8}$$

It was previously assumed that chemical weathering beneath ice sheets would be insignificant, as the bed would be frozen and isolated from the atmosphere [65], also leading to the assumption that these environments would be devoid of life. However, subsequent studies of GrIS outlet glaciers show complex geochemical signatures, evolving over the melt seasons and with solute concentrations comparable to smaller alpine glaciers [3,4,50,56,66,67], with microbial signatures providing evidence for complex biogeochemical reactions [68–72]. Bacterial activity has been shown to impact the rate of dissolution of amorphous silica phases [73] and microbial processes play an important role in solute acquisition where the combination of unfrozen bed, suitable redox conditions and sufficient concentrations of carbon substrates and other nutrients permits the existence of an active subglacial ecosystem. Weathering regimes in large ice sheet systems appear to differ from smaller alpine glaciers, which could be a result of differences in water residence time, catchment size and drainage system dynamics. Wadham *et al.* [56] outline a predictive framework of subglacial chemical weathering processes by using data from a range of glacial systems of varying size, to demonstrate the role of ice mass and water residence time on the predominant geochemical reactions, and the chemical composition of exported meltwaters. Greater isolation and longer subglacial water residence times can occur in larger systems, which can lead to the enhancement of silicate dissolution due to calcite saturation or exhaustion of calcite minerals by prolonged weathering [56]. This is likely to be different from smaller glacial systems, where carbonate dissolution dominates, and saturation or exhaustion of calcite minerals is not observed to the same degree. This is true in spite of bedrock, as seen in many small glacial catchments (e.g. Engabreen, Haut Glacier d'Arolla and Lemon Creek Glacier [56,57,64,74]). In these systems silicate-rich bedrock exists but coupled carbonate dissolution–sulfide oxidation still dominates chemical weathering [56,74], owing to the exposure of trace carbonates from bedrock via physical erosion.

More recent work by Graly *et al.* [55] suggests that the response of subglacial chemistry to changing water residence times is varied, probably because of the complex controls exhibited from a wide range of glaciological features, and atmospheric gas (CO_2 and O_2) and sediment supply, which play an important role in spatial and seasonal characteristics of subglacial geochemistry. These authors use data from a range of glaciers to provide evidence that the abundance of atmospheric gas at the bed, primarily from surface melt [75], results in carbonation being the dominant subglacial process [55]. Freshly comminuted sediment is also important for subglacial weathering processes, as the availability of fresh mineral surfaces and trace reactive

components impacts the proportion of easily dissolvable minerals (such as carbonates) within subglacial environments [55].

The hydrochemistry of the Watson River and specifically Leverett Glacier (LG), west Greenland, has been well studied owing to the large hydrologically active catchment size of LG (approx. 600 km^2) and its potential as a modern-day analogue for past ice sheets [50]. Hindshaw *et al.* [67] found low Ca^{2+}/Na$^+$ molar ratios (approx. 0.6) at LG, with elevated Na$^+$ and K$^+$ concentrations over Ca^{2+} and Mg^{2+} indicative of enhanced silicate weathering [56]. There are also characteristics of subglacial drainage that are more prevalent in large ice sheet catchments than in small valley glaciers. A good example is surface melt-driven subglacial outburst events in Greenland. 'Outburst events' occur during the ablation season at LG, and result in the flushing of the subglacial system via the rapid drainage of supraglacial lakes to the bed [62]. These outburst events result in elevated discharge, suspended sediment, pH and electrical conductivity, indicating they are flushing previously isolated areas of the subglacial system where water residence times may be significantly longer than those in areas of the bed accessed regularly or well connected to the existing hydrological drainage system [1,62]. The elevated Na$^+$ concentrations at LG coincide with outburst events during the melt season, which is consistent with the hypothesis of longer residence time waters with characteristics of enhanced silicate weathering. Hatton *et al.* [58] also found a switch from Ca^{2+} to Na$^+$ as the dominant cation in the meltwater river at LG as the melt season progressed and silicate weathering became the predominant weathering pathway.

Understanding the complex subglacial processes beneath large glacial systems is challenging, because of the difficulties around access and sampling logistics. We have used the subglacial reaction frameworks published previously [55–58], combined with measurements of δ^{30}Si composition in proglacial rivers, to produce a conceptual model of the subglacial processes impacting upon δ^{30}Si composition in the subglacial system (figure 1), in order to highlight the most important processes driving the exported δ^{30}Si composition. Figure 1 outlines the most likely subglacial weathering processes influencing δ^{30}Si$_{DSi}$ and δ^{30}Si$_{ASi}$ composition of glacial rivers, based upon current Si isotope measurements combined with hydrogeochemical data and concentrations of DSi, ASi and major ions. High physical erosion rates may be an important factor in determining δ^{30}Si$_{DSi}$ composition. Rock comminution results in fresh mineral surface layers enriched in isotopically light Si [76], potentially as ASi, however the formation mechanism for such is not well constrained, as discussed in §3c(ii). The dissolution of these mineral surface layers results in waters with an isotopically light δ^{30}Si$_{DSi}$ composition. If these areas of the subglacial environment are hydrologically connected with the main subglacial drainage system, then this signal is exported to the proglacial environment. We would therefore expect both small and large glacial catchments to export Si of isotopically light δ^{30}Si$_{DSi}$ composition, regardless of the dominant weathering regime, if we consider the relatively short-lived interactions between freshly comminuted surfaces and undersaturated meltwater, when hydrological drainage is efficient.

If we consider a large glacierized catchment then we can also consider the longer time-scale processes that could impact the δ^{30}Si$_{DSi}$ and δ^{30}Si$_{ASi}$ composition. We expect physical erosion and the dissolution of these isotopically light mineral surfaces to still be important in large systems when the subglacial hydrology is well developed, but we may also expect areas of subglacially stored waters with long residence times. In these long residence time waters it has been predicted that precipitation of secondary weathering products, such as ASi and potentially clays (discussed further in §3a), may occur as a result of supersaturation with respect to DSi (at least locally). Blackburn *et al.* [77] suggest that areas of low basal pressure result in the partial consumption of subglacial waters through local freezing, and cause solutes such as Si, Al, Fe and U to precipitate [77]. These secondary weathering products, such as ASi coatings, would be isotopically light, and subglacially stored waters would be enriched in heavier isotopes. However, if these areas of the bed then become hydrologically connected, further physical erosion and the addition of undersaturated waters during transport may occur. Therefore, these secondary weathering products may undergo redissolution, enriching the exported subglacial waters in isotopically

light Si. This means that the $\delta^{30}Si_{DSi}$ composition measured in proglacial rivers is always likely to be isotopically light, despite the potential for secondary mineral formation in isolated areas of the bed. This could potentially help to explain the isotopically light $\delta^{30}Si_{DSi}$ composition during outburst events at LG [58], when we expect the export of long residence time waters.

In smaller catchments we would expect a dominance of carbonate weathering processes and therefore the formation of secondary weathering products such as ASi and clays would be potentially reduced. It is therefore likely that this precipitation–redissolution process would be less prevalent in smaller systems with shorter residence times, meaning we might expect the light $\delta^{30}Si_{DSi}$ composition to mainly be driven by the interaction between freshly ground mineral surfaces and hydrologically connected undersaturated waters.

(c) Silicon fluxes from glacial systems

Complex subglacial geochemical processes, especially beneath large glaciers draining ice sheets, have the potential to export previously underappreciated fluxes of DSi and dissolvable ASi [2,7]. At present, we are limited by the small number of field studies, limiting the inferences we can make on subglacial weathering processes and potential nutrient fluxes presently and in the future. Furthermore, these environments are spatially and temporally heterogeneous, as illustrated by the GrIS, from which 80% of the total sediment is exported by only 15% of Greenlandic rivers [78].

Increasing focus has been placed on quantifying the fluxes of key nutrients from glacial systems [1,2,5,6,13,79,80] and understanding the weathering processes driving these fluxes [7,55–57,67,81–84]. Meltwaters from the GrIS contain DSi and ASi that may constitute significant fluxes of bioavailable Si into fjords and polar oceans. Meire *et al.* [5] estimated the export of DSi as $0.02\,Tmol\,yr^{-1}$, when upscaling data from two fjord systems and a range of glacial meltwater rivers. While this estimate is large relative to other nutrients, particulate Si associated with suspended sediment may increase this flux further. Hawkings *et al.* [2] considered both the dissolved and amorphous phases, resulting in a larger estimate of mean Si flux by an order of magnitude for the GrIS of $0.20\,(0.06-0.79)\,Tmol\,yr^{-1}$, approximately 50% of the input from Arctic rivers, with ASi accounting for greater than 95% of this flux. Dissolution experiments have shown this ASi to be highly soluble in seawater [2], consistent with laboratory studies of both biogenic and synthetic amorphous phases [85]. Therefore, it is likely that this Si is either directly or indirectly bioavailable (as DSi or ASi respectively) and could therefore stimulate the growth of diatoms and influence primary production. These findings are significant when considering the potentially high export of suspended sediments from the GrIS [86]; Overeem *et al.* [78] calculate that up to $1.28\,Gt\,yr^{-1}$ of suspended particulate matter (SPM) from the GrIS is entering the surrounding oceans. This agrees well with estimates of SPM export from the GrIS derived from LG; Hawkings *et al.* [2] estimated a maximum GrIS SPM export of $1.7\,Gt\,yr^{-1}$, with a more conservative mean estimate of $0.49\,Gt\,yr^{-1}$. However, the extent to which dissolved nutrients and those associated with this SPM reach surface and open ocean waters may be limited by nutrient drawdown and burial within complex fjord systems (see §4).

The export of Si from glacierized catchments varies (electronic supplementary material, table S1) and this is likely to be a result of varying subglacial conditions and reactions, as described in §1b. The purpose of the compilation in this review paper is to demonstrate Si yields from various glacial systems measured thus far, and to highlight the potential glacial systems have for contributing to regional biogeochemical cycles through the export of Si. Silicon yields were calculated according to equation (1.9) and Si concentrations, discharge and catchment size were compiled from a range of published studies.

$$\text{Si yield (ton km}^{-2}\text{a}^{-1}) = \frac{Q \times Q_{wt}\text{Si}}{\text{Catchment area}}$$
Where:
Q = annual discharge (l) \hfill (1.9)
$Q_{wt}\text{Si}$ = discharge-weighted Si concentration
Catchment area = glacial catchment size (km^2)

2. Methods to characterize Si in glacial meltwaters

To expand the existing dataset and provide a broader perspective into the δ^{30}Si composition of glacial meltwaters, we present new observations from 20 glaciers from across the Arctic and sub-Arctic (electronic supplementary material, table S2; figure 2). New samples were collected from August 2015 to September 2017 from glaciers corresponding to one of five major regions (Qeqertarsuaq (Disko Island), Iceland, Norway, Alaska and Svalbard), and each glacier was spot sampled once due to logistical restrictions.

There are currently some differences in how the community collects and analyses samples for δ^{30}Si composition, so we attempt to compile the range of methods currently in use (table 1), alongside describing the methods we employ. We highlight any differences and assess the potential implications of these discrepancies.

(a) Filtration

There are various ways to prepare water samples for Si isotope composition analysis (table 1) and this could have potential implications when considering the data produced. There is currently no standard protocol for filtration (e.g. filter membrane size, commonly 0.45 µm or 0.22 µm, and/or filter type), although different membrane types are used to aid with sampling large volumes of water, or water high in suspended particulate phases. This lack of standardization has the potential for introducing bias if significant proportions of the total Si are held within colloidal or nanoparticulate size fractions, relative to the truly dissolved phase. Currently, both depth and screen membrane filters are used in the field. Depth filters have layers of randomly orientated fibres that make up the filter, and usually have a pore size rating determined from bubble point tests. Screen membrane filters (e.g. track etched polycarbonate) do not pass anything larger through than the stated pore size (measured by visual examination) by performing separation on the surface of the membrane. Morrison & Benoit [91] found that colloids of Fe, Al, Mn and organic carbon behaved differently when comparing the impact of filter clogging of different elements and that it cannot be assumed that a clogged filter is necessarily trapping the same proportion of colloidal phases of all elements. Depth filters can initially trap size fractions smaller than the specified filter size by adsorption but are less likely to clog and trap smaller particle sizes as filtration progresses. By contrast, screen filters clog more rapidly, with the effective pore size reducing progressively [92], and there is a strong correlation between increasing back pressure and decline of colloidal concentrations [91]. There is therefore a difficult balance between initially passing sample through the filter for a preliminary wash and to flush out any residual cleaning acid, filling any potential adsorption sites in the membranes and clogging up the filter membrane. This is especially critical with samples such as glacial meltwaters where the sediment load is high (commonly greater than $1 \, \mathrm{g \, l^{-1}}$) and the effective pore size reduces quickly [92]. These issues present potential implications, considering that different filter membranes are used across research projects, which could alter the conclusions drawn about the truly dissolved δ^{30}Si composition. The influence of filter membrane type on colloidal and nanoparticulate Si [2] has not yet been explored systematically in the field or experimentally.

(b) Sampling methodology

The new data we present in this study (electronic supplementary material, table S2; figure 2) followed the methods reported in Hawkings *et al.* [50] and Hatton *et al.* [58]. Briefly, samples were collected using clean Nalgene bottles (high-density polyethylene—HDPE) and filtered immediately in the field through 47 mm 0.45 µm cellulose nitrate membrane filters (most similar in behaviour to the depth filters described above). The filtrate was kept refrigerated at 4°C in the dark until analysis. The filters were retained, kept refrigerated in the dark, and transported back to the laboratory and air dried in a laminar flow hood.
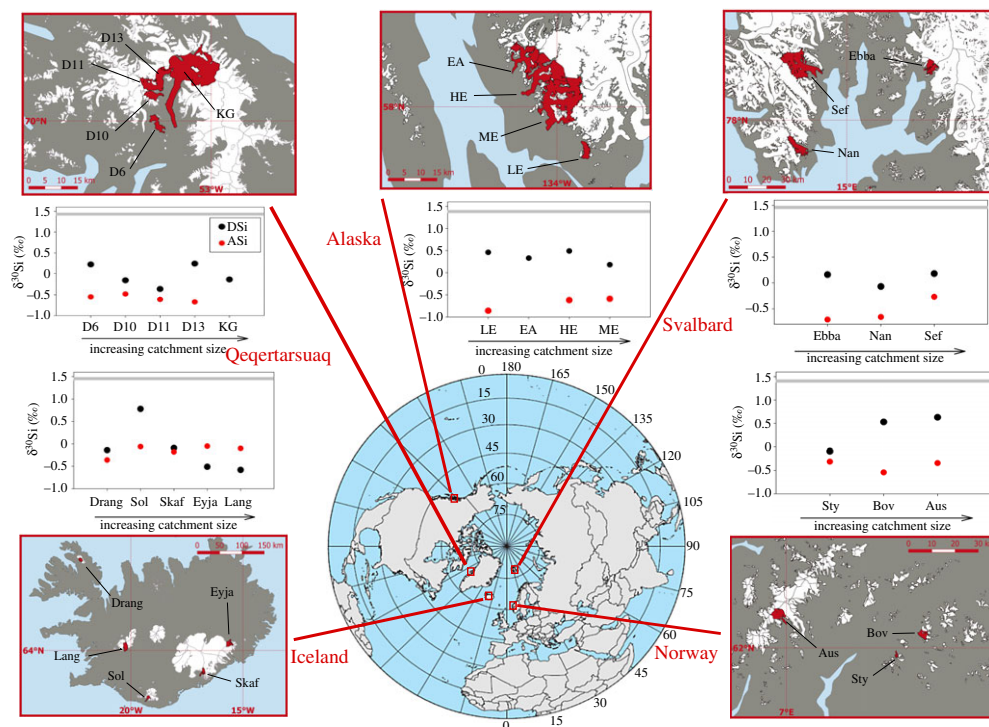
Figure 2. Location map of glacial rivers analysed for the silicon isotope (δ^{30}Si) composition for dissolved (DSi) and amorphous (ASi) phases. The proglacial rivers of the glaciers highlighted in red in the five smaller maps were sampled for δ^{30}Si composition. Clockwise from lower left; Iceland, Qeqertarsuaq (Disko Island), southeast Alaska, Svalbard and Norway. Graphs show the δ^{30}Si$_{DSi}$ (black) and δ^{30}Si$_{ASi}$ (red) composition measured for each glacier, organized by location. Error bars, mainly included in the symbol size, represent average external errors (0.08‰, 2 s.d.). Glaciers are organized by catchment size on each graph (acronyms defined in electronic supplementary material, table S2). The horizontal grey line represents the average non-glacial δ^{30}Si$_{DSi}$ composition compiled from published data (see figure 3 for references). (Online version in colour.)

Table 1. Compilation of published methods for sample collection and storage for the analysis of silicon isotope composition from rivers.

| study | location | sample collection | | time before | storage |
		filter size (µm)	filter type	filtering	
Hawkings *et al.* 2018 [50]	Leverett, Greenland	0.45	cellulose nitrate	immediately	refrigerated in field
Opfergelt *et al.* 2013 [44]	Iceland	0.2	cellulose acetate	<24 h	
Georg *et al.* 2006 [43,87]	Switzerland	0.45	cellulose acetate	immediately	acidified with HCl
Georg *et al.* 2007 [49]	Iceland	0.2			acidified with HNO$_3$
Ding *et al.* 2004 [88]	Yangtze River, China	not specified	not specified	<2 weeks	refrigerated
Ding *et al.* 2011 [89]	Yellow River, China	not specified	not specified	<24 h	
Cardinal *et al.* 2010 [46]	Congo River	0.2	cellulose acetate		refrigerated; acidified with conc. HNO$_3$
Hughes *et al.* 2013 [90]	Amazon River	0.22	cellulose nitrate		

We ensured all samples reported in this study used the same filter types as those in previous studies of Greenlandic meltwaters [50,58], so we could confidently compare the data. However, other studies have used different filter types and different pore sizes (for example Opfergelt *et al.* [44] used 0.2 µm cellulose acetate filters), resulting in potential differences in what is defined as the truly dissolved phase when $\delta^{30}Si_{DSi}$ composition is discussed.

(c) Sample preparation for Si isotope analysis

Water samples for $\delta^{30}Si_{DSi}$ were evaporated so that approximately 2 ml of sample had a concentration of approximately 2 ppm. This sample was subsequently passed through a pre-conditioned BioRad AG 50 W-X12 cation exchange resin for purification [87]. Suspended sediments from the filters (for $\delta^{30}Si_{ASi}$) were extracted by the addition 0.2M NaOH for 40 min at 100°C. This extraction method was used as it targets the amorphous silica phase [93], which will complement ASi concentration data. Samples were then neutralized with 8N HNO_3 and passed through a similar pre-conditioned BioRad cation exchange resin as for water samples.

Silicon isotope analysis was carried out in the Bristol Isotope Group laboratories (University of Bristol, UK) using a Thermo Scientific™ Neptune High Resolution Multicollector inductively coupled plasma mass spectrometer (MC-ICP-MS), using a standard-sample-standard bracketing procedure, using the international reference standard NBS-28 (NIST RM8546, purified quartz sand). Samples were also doped with intensity-matched Mg solution to correct for internal mass bias and 100 µl of 0.1M H_2SO_4 to account for potential anionic matrix mass bias [50,94].

3. Silicon isotope composition of glacial rivers

(a) Theoretical isotopic composition of DSi

Glaciers are highly effective physical erosion agents. The process of rock comminution results in an abundant supply of fine-grained rock flour, exposure of trace reactive components in the bedrock, modification of mineral surfaces and subsequent chemical weathering, all of which are likely to influence the composition of meltwaters exported from the glacier. Our knowledge of the fractionation of Si isotopes during low-temperature surface processes allows predictions of the dissolved isotopic signature of glacial meltwaters. If indeed silicate mineral weathering is enhanced beneath large glacier systems, then we might expect a fractionation effect which enriches the residual meltwater in the heavier isotopes (due to preferential uptake of ^{28}Si) during the formation of secondary weathering products, such as clays. The high pH within subglacial environments [7,58] and highly reactive nature of SPM favours secondary mineral precipitation, with reaction path models showing that subglacial water chemistries cannot be balanced when only considering dissolution processes [95]. However, subglacial clay formation is uncertain, with differing interpretations based upon proglacial meltwater and borehole chemistry [7,43,95,96]. For example, analysis of glacial rivers in west Greenland found that waters were undersaturated with respect to almost all clay minerals and X-ray diffraction showed no obvious signs of secondary clays [96], but it is unknown whether this is typical of all glacial catchments. $\delta^{30}Si_{DSi}$ composition alone cannot currently be used to inform on clay formation, owing to repeated dissolution and reprecipitation cycles impacting upon isotopic fractionation and the differences in fractionation factors between different clay minerals [20,97,98]. The first smaller scale studies of $\delta^{30}Si_{DSi}$ composition comparing glacial versus non-glacial riverine systems did not fully support the subglacial clay formation. Opfergelt *et al.* [44] analysed 18 river samples from glacierized catchments and non-glacierized catchments in Iceland and reported that the non-glacial rivers have a heavier $\delta^{30}Si_{DSi}$ composition than the glacial rivers (+0.97±0.31‰, compared with +0.17±0.18‰). The $\delta^{30}Si_{DSi}$ compositions measured in the non-glacial rivers were consistent with a supply-limited regime, with clay formation preferentially incorporating the light isotopes, resulting in heavier $\delta^{30}Si_{DSi}$ composition. They inferred that the $\delta^{30}Si_{DSi}$ compositions measured in the glacial rivers followed a so-called kinetically limited regime, with Si from the basaltic

bedrock undergoing dissolution in relatively high pH conditions, but the extent of the weathering being insufficient to permit extensive clay mineral formation [44].

Consistent with this initial finding on rivers draining small Icelandic glaciers, Hawkings *et al.* [50] and Hatton *et al.* [58] also found a consistently light $\delta^{30}Si_{DSi}$ composition when completing a seasonal study of subglacial run-off from LG. LG has a much larger hydrologically active catchment (approx. $600\,km^2$) than most of the glaciers studied in Iceland, and the $\delta^{30}Si_{DSi}$ composition was lighter on average than both the glacial Icelandic rivers and non-glacial rivers measured previously (discharge-weighted mean of $-0.25‰$). Variations in $\delta^{30}Si_{DSi}$ composition alongside the major ion chemistry of run-off indicated a direct correlation between the $\delta^{30}Si_{DSi}$ composition and the extent of silicate mineral weathering as inferred from ratios of Na^+/Ca^{2+} and divalent/monovalent ions. By mid-melt season, when flow paths are longest, Hatton *et al.* [58] reported an isotopic signature of $-0.52‰$ at LG, which was the lightest $\delta^{30}Si_{DSi}$ composition measured in running waters to date. Investigation of a smaller Greenlandic glacier found a $\delta^{30}Si_{DSi}$ composition lighter than non-glacial river waters, but not as light as the $\delta^{30}Si_{DSi}$ composition measured at LG, leading to the hypothesis that the larger catchment undergoes enhanced silicate mineral weathering, as a result of more isolated subglacial waters with longer residence times, driving the lighter $\delta^{30}Si_{DSi}$ composition [58], as discussed further in §3b(ii).

(b) New DSi isotopic data: what do we learn from an expanded dataset?

(i) Contribution of glacial rivers to global isotopic mass balance

In order to assess the isotopic composition of glacial meltwaters more widely, the present study incorporates new data from 20 Arctic and sub-Arctic glaciers (electronic supplementary material, table S3), which range in geographical location, bedrock lithology, catchment size, subglacial hydrological and weathering regime. Considering a wider range of proglacial rivers will help to quantify the average glacial melt-fed river $\delta^{30}Si_{DSi}$ composition and assess the patterns and hypotheses drawn from the existing data.

The $\delta^{30}Si_{DSi}$ composition for all the glacial rivers measured is consistently lighter than the non-glacial average (figure 3). The sample from Langjökull (west Iceland) has the lightest $\delta^{30}Si_{DSi}$ composition measured in running waters ($-0.58‰$), lower (but statistically within error) than the lightest value reported from LG in 2015 during a subglacial outburst event ($-0.52‰$ [50]). It is important to note that Langjökull was sampled during a heavy rainfall event, which could have had an impact on the meltwater chemistry. However, sampling was completed very close to the glacier terminus and light $\delta^{30}Si_{DSi}$ composition was measured at other Icelandic glaciers (e.g. Eyjabakkajökull, $-0.51‰$) when weather conditions were dry and sunny.

The light $\delta^{30}Si_{DSi}$ compositions measured from the new glaciers presented in this paper are consistent with findings from Georg *et al.* [49], Opfergelt *et al.* [44], Hawkings *et al.* [50] and Hatton *et al.* [58], indicating that subglacial weathering processes are the primary cause of the light $\delta^{30}Si_{DSi}$ composition exported from these environments. The $\delta^{30}Si_{DSi}$ composition from the Watson River in September 2017, which is fed by three outlet glaciers from the GrIS, including LG, was $+0.31‰$. This indicates that LG likely exports isotopically light DSi throughout the melt season, until shut-down of the hydrological system, which concurs with calculations by Hatton *et al.* [58]. This value is heavier than the $\delta^{30}Si_{DSi}$ composition measured at LG during the peak melt season. This could potentially reflect mixing between waters of different origin, rather than a shift in subglacial weathering processes, as the Watson River is more influenced by non-glacial water sources than the LG proglacial river. Additionally, one of the outlet glaciers feeding the Watson River is Russell Glacier, which is a small outlet glacier with currently uncharacterized $\delta^{30}Si_{DSi}$ composition. But we may expect the $\delta^{30}Si_{DSi}$ composition from this glacier to be isotopically heavier than that of LG, based on the comparison of Greenland catchments by Hatton *et al.* [58]. Alternatively, assuming the hypothesis that isotopically light $\delta^{30}Si_{DSi}$ composition is driven by mechanochemical reactions is correct, then we might expect to see an increase in $\delta^{30}Si_{DSi}$

13

royalsocietypublishing.org/journal/rspa Proc. R. Soc. A **475**: 20190098
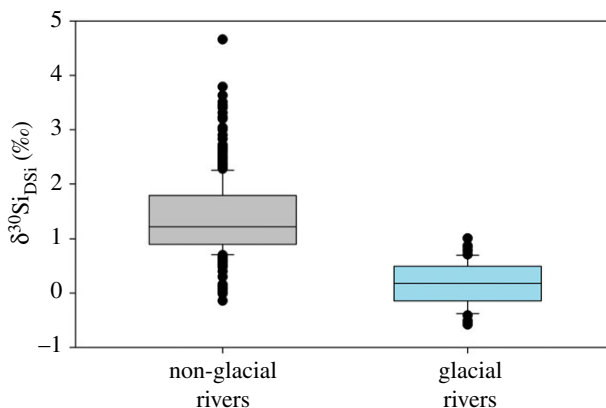
Figure 3. Box plot showing the global average dissolved silicon isotope ($\delta^{30}\text{Si}_{\text{DSi}}$) composition from glacial and non-glacial rivers. Data compiled from existing published sources [44,49,50], from this study for glacial rivers (+0.16‰) and from published sources for non-glacial rivers (+1.38‰) [37,43–46,88–90,99–105]. Boxes represent upper and lower quartiles, with the median represented by the middle line. (Online version in colour.)

composition as glacial motion and rock grinding slows later in the season. This is consistent with the increasing $\delta^{30}\text{Si}_{\text{DSi}}$ composition at the end of the monitoring period at LG in 2015 [50,58].

An updated database of non-glacial rivers provides a mean $\delta^{30}\text{Si}_{\text{DSi}}$ composition of +1.38‰, compared with the previous estimates of +1.25‰ by Frings *et al.* [17] [37,43–46,88–90, 97,99–105]. This compares with a mean $\delta^{30}\text{Si}_{\text{DSi}}$ composition of glacial rivers of +0.16‰, based on the new glaciers reported in this study and glacial rivers published previously [44,49,50]. Note, in the absence of Si concentration data, discharge data and/or a seasonal record of $\delta^{30}\text{Si}_{\text{DSi}}$ composition for many rivers we have reported a simple mean value.

(ii) Controls of $\delta^{30}\text{Si}_{\text{DSi}}$ composition of glacial meltwaters

Statistical analyses of these data, such as regression model and principal component analysis, do not reveal any significant relationships to suggest an overriding process that is the main cause of the light Si isotopic composition in glacial meltwaters. This is likely to be due to the complex nature of subglacial processes and the temporal development of the hydrological system (and associated biogeochemical conditions) over a melt season [59,62,66,106]. Evidence from the limited number of Greenlandic catchments that have been monitored over a melt season suggests that changes in subglacial weathering regime, associated with hydrological evolution from an inefficient subglacial drainage system to an efficient channelized drainage system, influences the $\delta^{30}\text{Si}_{\text{DSi}}$ composition of exported waters [58]. $\delta^{30}\text{Si}_{\text{DSi}}$ composition generally decreased over the melt season, with the lowest $\delta^{30}\text{Si}_{\text{DSi}}$ composition coinciding with outburst events at LG and the hydrological connection of the subglacial system at a smaller Greenlandic catchment, Kiattuut Sermiat (KS) [58]. We postulate that this pattern would also be seen in other glacial systems, had it been possible to monitor a larger range of glaciers over a longer time period rather than treating samples from all the glaciers as a single dataset.

There are currently various hypotheses for explaining the light $\delta^{30}\text{Si}_{\text{DSi}}$ composition in glacial meltwaters. On the basis of evidence from Greenlandic glacial systems, Hawkings *et al.* [50] hypothesized that glaciers with a larger catchment size would export meltwaters with a lighter $\delta^{30}\text{Si}_{\text{DSi}}$ composition. These authors suggest that the isotopically light amorphous mineral surface layers, which form through precipitation or leaching in a long residence system, subsequently undergo redissolution (due to high pH and undersaturation of waters with respect to ASi), resulting in a lighter $\delta^{30}\text{Si}_{\text{DSi}}$ composition [50]. However, analysis of $\delta^{30}\text{Si}_{\text{DSi}}$ composition from the wider range of glaciers presented in this study shows no significant relationship between
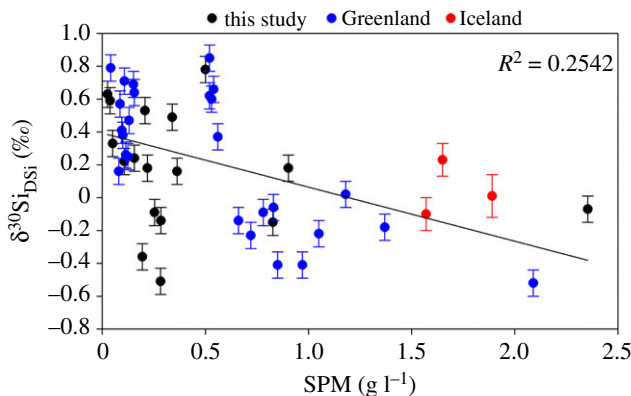
Figure 4. Relationship between suspended particulate material (SPM) concentrations and the dissolved silicon isotope ($\delta^{30}Si_{DSi}$) composition of glacial meltwaters. Data are reported from glaciers measured in this study, Greenland [50,58] and Iceland [44]. Data have been trimmed to remove outliers (95th percentile), and the regression line has an R^2 value of 0.2542. Error bars on data from this study represent the average external error of 0.08‰ (2 s.d.), based on triplicate measurements of a subset of samples. (Online version in colour.)

$\delta^{30}Si_{DSi}$ composition and catchment size, with glacierized catchment area ranging from 1.5 to 131 km^2. This may be because of the challenges in assessing the size of the hydrologically active catchment area when the sample was taken from the proglacial river, and the lack of a clear relationship between catchment size and water residence time. It may also suggest that $\delta^{30}Si_{DSi}$ composition of glacial meltwaters is not directly driven by catchment size, but potentially by a range of factors in addition to subglacial water residence times, such as physical erosion processes (e.g. mechanochemistry). We also postulate that differences in bedrock lithology would not result in significant variations in $\delta^{30}Si_{DSi}$ composition [58], as high-temperature processes produce limited isotope fractionation and the $\delta^{30}Si$ composition of crustal silicate rocks is relatively homogeneous [107,108].

The very high rates of physical erosion in subglacial environments could also be considered the main driver for light $\delta^{30}Si_{DSi}$ composition in glacial meltwaters, as discussed previously. Elevated physical erosion rates result in the formation of finely ground, reactive glacial flour and exposure of trace reactive minerals with very high surface areas [78,81,86,109,110]. This process is also a potential mechanism for formation of isotopically light ASi [76], as discussed in §3c(ii). There is likely to be preferential leaching of ^{28}Si from these freshly ground mineral surfaces, resulting from kinetic fractionation, as demonstrated by dissolution experiments on Hawaiian basalts [76]. Dissolution conditions are favourable in the subglacial environment, despite the low temperatures, owing to the high pH (from hydrolysis of freshly ground carbonate and silicate minerals) and undersaturation of meltwaters with respect to ASi. There is some indication that higher suspended sediment concentrations are linked to lighter $\delta^{30}Si_{DSi}$ composition in glacial meltwaters, with the lightest $\delta^{30}Si_{DSi}$ values measured either during the outburst events at LG (categorized by SPM of 1–2 g l^{-1}) or from Langjökull (where SPM was extremely high, at approx. 47 g l^{-1}; figure 4). However, we have chosen to remove the SPM data from Langjökull from our analysis as this site was sampled during a very heavy rainfall event, and therefore the measured SPM is not likely to be representative of baseflow conditions.

The role of permafrost in modifying $\delta^{30}Si$ composition of glacial streams has not been considered for the data presented in this review paper as all of the rivers have been sampled close to the glacier front. However, the impact of weathering reactions within permafrost active layers should not be overlooked if river samples are taken further from the subglacial outflow. The impact of permafrost on riverine $\delta^{30}Si$ composition is relatively understudied at present but evidence suggests that seasonal changes in $\delta^{30}Si$ composition of streams occur as a result of seasonal permafrost changes [97,102,111]. For example, the $\delta^{30}Si_{DSi}$ composition of the Lena River

decreases from winter to summer. This is likely to be due to the dominant winter Si source being from intrapermafrost layers with enhanced clay formation, whereas the summer Si is sourced from permafrost upper active layers where dissolution of silicate minerals and phytoliths occurs [97]. Therefore, it is important to consider the potential role of permafrost on Si flux from high-latitude rivers and upon the 'glacial' riverine $\delta^{30}Si_{DSi}$ composition, especially under climatic warming scenarios and the predicted associated permafrost thawing.

(c) Glacially derived amorphous silica

(i) Contribution of glacial amorphous silica to global budgets

The export of Si from glacial systems is dominated by the reactive ASi fraction, with the mean ASi concentrations in glacial rivers being significantly higher than from other riverine systems (e.g. mean ASi concentration of 392 µM from LG [2]). It is therefore important to investigate the isotopic composition of glacial ASi and improve our understanding of the formation and eventual fate of this fraction. Hawkings *et al.* [50] presented the first data on the $\delta^{30}Si_{ASi}$ composition of riverine waters, analysing suspended sediments over a melt season from LG. This was followed by a study comparing two catchments, LG and KS in Greenland [58]. $\delta^{30}Si_{ASi}$ composition in Greenland was light and relatively uniform for both catchments, consistently approximately 0.2‰ lighter than the bulk bedrock measurements of the catchments. $\delta^{30}Si_{ASi}$ composition was generally lighter than the $\delta^{30}Si_{DSi}$ composition (by 0.02 to +0.82‰ at LG and by 0.68 to +1.27‰ at KS), except for outburst events at LG, when the $\delta^{30}Si_{DSi}$ composition was lighter by 0.37‰.

The new glaciers presented in this study (with the exclusion of Langjökull, owing to the extreme SPM mentioned previously) have a $\delta^{30}Si_{ASi}$ composition in the range of −0.05‰ to −0.86‰, with an SPM normalized average of −0.27‰. As no discharge data are available for the glaciers sampled, we used the suspended sediment concentration (in $g\,l^{-1}$) to weight the $\delta^{30}Si$ values, as this is the only common parameter available from all glaciers measured to enable a weighted mean. The SPM varies from 0.01 to $2.35\,g\,l^{-1}$ with an average of $0.39\,g\,l^{-1}$, and an average ASi concentration of 0.5 dry wt.% (0.09–2.1 dry wt.%). This is similar to the current mean ASi of global rivers (0.6 wt.% [17]). The average $\delta^{30}Si_{ASi}$ composition of these new glacierized catchments is similar to the discharge-weighted (Q_{wt}) mean $\delta^{30}Si_{ASi}$ composition of a large Greenlandic catchment, LG (−0.22‰). Kiattuut Sermiat had a lighter Q_{wt} mean $\delta^{30}Si_{ASi}$ composition of −0.47‰ [58], which is still within the range of values measured across these other glaciers. It is difficult to directly compare these values as the averages are not calculated with the same weighting (discharge-weighted mean versus weighted by suspended sediment concentration). There is no statistically significant relationship between $\delta^{30}Si_{ASi}$ composition and SPM ($R^2 = 0.0048$, $p = 0.5278$) when looking at the dataset as a whole, however there appears to be a general increase in $\delta^{30}Si_{ASi}$ composition as catchment area and ASi concentration increase. Whilst these relationships are not statistically significant ($R^2 = 0.4149$, $p = 0.0657$ and $R^2 = 0.3809$, $p = 0.0508$, respectively; figure 5) they provide an interesting trend, and the data are complicated by lack of seasonal catchment records, which is likely to be causing the lack of a significant relationship.

The range of $\delta^{30}Si_{ASi}$ compositions measured across these glaciers is also consistent with data presented from non-glacial rivers. Ding *et al.* [88] report an average $\delta^{30}Si$ composition of SPM in the Yangtze River of −0.34‰ (with a range of 0‰ to −0.7‰) and Ding *et al.* [89] present an average $\delta^{30}Si$ composition of −0.02‰ (0.3‰ to −0.4‰) for SPM in the Yellow River. However, it must be considered that these values are calculated from the total SPM, using total digests, which probably results in the inclusion of other clay minerals rather than a measurement of only the ASi phases. It is also likely that the $\delta^{30}Si$ composition of SPM in these systems is significantly impacted by phytolith contributions, owing to the variable range of $\delta^{30}Si$ composition that phytoliths exhibit [18,88,112]. None of the ASi within the highly turbid proglacial rivers measured is expected to be biogenic; the low temperatures, high SPM loads and subglacial origin indicate the environment is not conducive for primary producers.
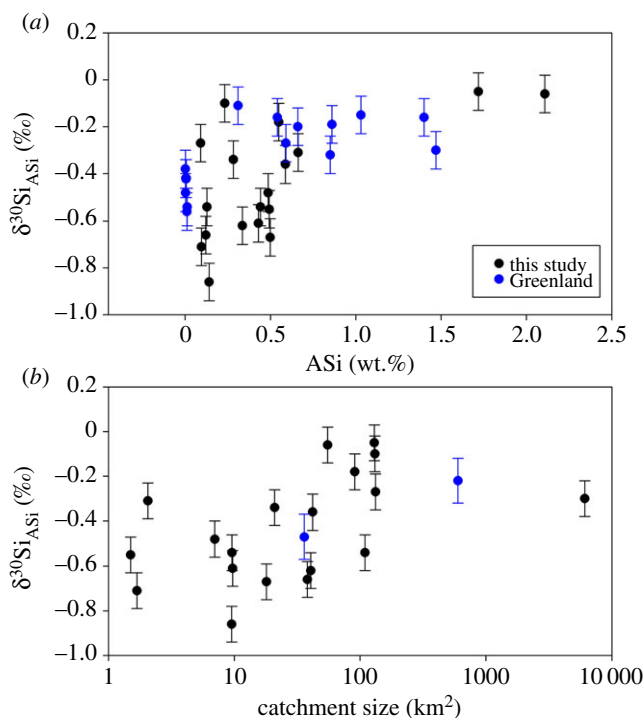
Figure 5. Relationships between catchment size and amorphous Si (ASi, wt.%) and the silicon isotope ($\delta^{30}Si_{ASi}$) composition in suspended particulate matter of the new glacial meltwaters analysed in this study and from Greenland [58]. Error bars represent an average external error of 0.08‰ (2 s.d.), based on triplicate measurements of standards and a subset of samples, except for the Greenlandic samples in (*b*). These datapoints represent the discharge-weighted mean $\delta^{30}Si_{ASi}$ composition from measurements over the ablation season and error bars represent the range of values measured over the season. (Online version in colour.)

Assuming simple mass balance, glacial $\delta^{30}Si_{ASi}$ composition should be heavier than that in non-glacial rivers to offset the light $\delta^{30}Si_{DSi}$ composition of these meltwaters. However, the Si pool in subglacial systems is so large that the export of isotopically light DSi does not have a significant impact upon the overall isotopic composition of the ASi reservoir. A simple fractionation model illustrates that less than 5% of the measured ASi is needed to undergo dissolution to produce the lightest $\delta^{30}Si_{DSi}$ composition (-0.56‰ at LG [58]).

(ii) Controls of $\delta^{30}Si_{ASi}$ composition from glacial sources

High-resolution transmission electron microscope photomicrographs show the presence of amorphous silica nanostructures in SPM from Greenland and iceberg-entrained debris [2]. The origin of ASi from glacial environments is not yet constrained, making it challenging to assess the Si isotope fractionation process during its formation. However, we can assume that the light $\delta^{30}Si_{ASi}$ composition results from low-temperature fractionation associated with the enhanced physical and chemical weathering that occurs in subglacial systems. Two chemical weathering hypotheses for the formation of ASi have been proposed: the leached surface layer hypothesis and the dissolution–reprecipitation mechanism [2]. The leached surface layer hypothesis describes the dissolution of weakly bonded ions, resulting in the formation of amorphous crusts enriched in less soluble ions, such as silicon. The dissolution–reprecipitation hypothesis predicts the dissolution of the finely ground mineral surface layer and then the formation of ASi through the reprecipitation of silica due to supersaturation at the grain boundary [2,113].

A separate hypothesis is based on mechanochemical reactions from glacial bed grinding, whereby ASi is generated from a disturbed surface layer. These physical processes impact the structure of mineral surfaces [2,68], and result in the formation of surficial amorphous layers, with structural changes, lattice distortion and associated chemical changes [114,115]. Preferential dissolution of ^{28}Si from these freshly ground mineral surfaces occurs due to kinetic fractionation [76], driving the system towards lighter $\delta^{30}Si_{DSi}$ compositions by around $-1‰$.

Both physical and chemical weathering hypotheses for the formation of ASi result in isotopically light ASi, so analysis of SPM using Si isotopes alone will not help to distinguish the most likely formation mechanism. Photomicrographs of ASi nanostructures in sediments from Greenland and iceberg-entrained debris show that the ASi is mainly associated with the edges of other material, and electron diffraction spectroscopy indicates that less soluble elements such as Fe and Al are incorporated into its nanostructure [2]. While this means its formation could be a result of both aluminosilicate mineral weathering and/or mechanical grinding, novel high-resolution microscopic and spectroscopic techniques to investigate these structures and associated elemental characteristics may provide a way to distinguish between subglacial chemical and physical weathering processes in the future. Furthermore, it may be useful to conduct controlled laboratory experiments to mimic the subglacial system. For example, erosional processes could be simulated through rock crushing and dissolution could be traced using a combination of isotopic analyses and major ion concentrations and composition.

4. Wider impact of glacial Si

Glaciers have been associated with high nutrient fluxes, including Si in dissolved and dissolvable amorphous forms [2]. However, an important outstanding question is how much of this exported material reaches the open ocean, especially from the GrIS, where complex fjord networks exist.

(a) Fjords as conduits of Si to the marine system

Upwelling of marine-sourced nutrients has generally been considered to dominate inputs to high-latitude fjords, both along the West Antarctic Peninsula [116] and in Greenland fjords [117]. However, glacially exported nutrients might have an important impact on biogeochemical cycles within fjord systems [2,13,118–120]. Furthermore, upwelling marine waters are likely to have been modified by inputs (e.g. of Si and Fe) from shelf sediments, which are composed of recently deposited glacially derived material [121–123].

In Greenland, Si concentrations are elevated in fjords in front of both land-terminating and marine-terminating glaciers as a result of meltwater input [5,124]. Young Fjord (with melt input from a land-terminating glacier) displayed a dominance of diatoms over other phytoplankton species, probably because of the increased availability of DSi from glacial meltwaters [5]. In Godthåbsfjord (with inputs from marine- and land-terminating glaciers), the upwelling of subglacial discharge led to sustained phytoplankton blooms with high Si:N ratios, resulting in a diatom-dominated summer phytoplankton assemblages (up to 95%). Hawkings *et al.* [2] also found elevated DSi concentrations within a sediment-rich plume in the surface waters of a Greenlandic fjord, which directly correlated with salinity. This is unlikely to be explained solely by mixing between fresh and marine end-member waters. A simple leaching experiment carried out by Hawkings *et al.* [2] showed that ASi in SPM of Greenlandic sediments undergoes dissolution in sterile marine waters, releasing bioavailable DSi. Although the DSi profile observed by Hawkings *et al.* [2] appears fairly unusual compared with other fjords sampled, this observation, combined with elevated ASi dissolution rates in marine water, highlights a role of amorphous silica in fjord and near-coastal Si budgets, and could help to explain at least part of the elevated DSi concentrations within the sediment plume. This is also in agreement with studies which suggest that riverine particulate material dissolves upon arrival to the ocean, as explanation of the Si fluxes and oceanic $\delta^{30}Si_{DSi}$ composition [125].

The fate of glacially exported Si beyond fjords and in the coastal zone, however, is uncertain. Fjords display complex physical, biological and chemical processes on various spatial and temporal scales [117], which could potentially trap glacially supplied nutrients and limit their impact on biogeochemical cycles beyond these fjords [13]. High nutrient consumption by diatoms within fjord systems is one of the most likely mechanisms that could limit the flux of dissolved nutrients into the open ocean [5,118,126]. It is also likely that high nutrient consumption will trap lighter isotopes in the solid phase, as found in brackish/estuarine diatom fractionation [127], meaning DSi would become increasingly isotopically heavy away from the glacial input source. Surface waters influenced by glacial meltwaters off the coastal shelf seas off southwest Greenland in summer 2017 were found to have low DSi concentrations [128]. The low Si may indicate that the dissolution of glacially derived suspended sediments is exceeded by the Si uptake rate of diatoms, or that the ASi fraction has been exhausted in the fjord environments and therefore the kinetics of the remaining Si would be much slower than the dissolution rates of the ASi, so the SPM may not impact the DSi in the ocean. However, these preliminary data also show that these areas of the coastal ocean have elevated turbidity, indicating that glacial suspended sediments could be reaching the coastal ocean, and could therefore still be a potential source of nutrients after further processing of suspended particles. In addition, remote sensing images reveal phytoplankton blooms extending over 300 km into the Labrador Sea, which coincide with addition of glacial meltwaters in south and southwest Greenland [6,129]. However, the mechanism driving these blooms has yet to be fully elucidated. The input of nutrients from glacial meltwaters, most likely Fe, into the ocean may help to stimulate phytoplankton growth, but the production could be linked more to physical processes, such as the increased stratification and mixed layer light levels, rather than nutrient supply *per se* [6,130]. While freshwater entering the open ocean travels hundreds of kilometres from its origin [6,131,132], further work is needed to fully quantify the fluxes of nutrients associated with this glacial meltwater into the open ocean before we can attempt to make firm conclusions around the impact of glacially derived nutrients on wider biogeochemical cycles.

(b) Impact on the global Si cycle of light Si isotopes from glacial meltwaters?

Despite the uncertainty surrounding nutrient cycling in fjords, it is clear that glacial meltwaters demonstrably reach the open ocean by mixing across continental shelves and are carried significant distances by boundary currents [128]. If glacially derived Si is entering the downstream Si cycle, we can postulate its impact on our current interpretations of oceanic Si cycling and the isotopic composition of the ocean. Glacial rivers export Si with a significantly lighter $\delta^{30}Si_{DSi}$ composition than non-glacial rivers, yet few Si models currently include glacial fluxes of Si and until recently assumed the $\delta^{30}Si_{DSi}$ composition of riverine input into the ocean is relatively constant over longer time periods [17]. This could be problematic considering the potentially important glacial Si flux, with the GrIS alone estimated to be 0.20 (0.06–0.79) Tmol yr^{-1} [2], compared with an estimated global riverine flux of Si of 7.3–8.1 Tmol yr^{-1} [17].

The 'missing' Si flux from glacial environments could be especially important when considering climatic change over glacial cycles. The isotopic composition of biogenic silica in marine sediment cores can be used as a palaeo-proxy to infer changes in the past Si cycle. For example, biogenic silica isotopic records from the Last Glacial Maximum (LGM) to present day reveal an increase in $\delta^{30}Si$ of around 0.5–1.0‰, with these findings consistent in the Southern Ocean, North Atlantic and Eastern Equatorial Pacific [17]. These changes have been interpreted as shifts in diatom utilization of silicic acid over glacial–interglacial periods, with lower utilization at the LGM than at present, as increased utilization would enrich surface waters in isotopically heavy Si [133,134]. However, this hypothesis assumes that the riverine input of $\delta^{30}Si$ into the oceans has been relatively consistent from the LGM to the present day in both flux and $\delta^{30}Si$ composition. In particular, many previous studies did not consider any impact from glacial meltwaters, which could have a distinct isotopic composition compared with non-glacial rivers [43,44,50].

At the LGM and during deglaciations the oceanic δ^{30}Si composition could have been impacted by light glacial δ^{30}Si$_{DSi}$ exported from palaeo-ice sheet. These fluxes are likely to have been greatest during Meltwater Pulse 1A and 1B (approx. 14 000–15 000 BP and approx. 11 000 BP, respectively). A simple box model, using the δ^{30}Si$_{DSi}$ and δ^{30}Si$_{ASi}$ composition of LG in Greenland as an analogue for North American and Eurasian ice sheets, showed that glacial systems may have shifted global oceanic δ^{30}Si$_{DSi}$ by 0.06–0.17‰, which accounts for 10–20% of the change in oceanic δ^{30}Si$_{DSi}$ since the LGM to present day [50]. In addition, data from a high-frequency sponge spicule core record close to Iceland show variability in δ^{30}Si composition of up to −0.6‰ over 300 years, coinciding with rapid Icelandic Ice Sheet collapse [50]. This rapid decrease in δ^{30}Si composition, of such a significant magnitude, suggests an influx of glacial meltwater perturbing the system. A rapid flux of isotopically light DSi would probably have been glacially sourced when considering the light δ^{30}Si composition measured across the range of glaciers, including those in Iceland (this study, Georg *et al.* [49] and Opfergelt *et al.* [44]). The Si inventory of the ocean is also expected to be larger during the LGM as a result of glacial fluxes, which could have wider implications for primary productivity and CO_2 drawdown [135]. A larger Si inventory also has the potential to shift the phytoplankton species assemblages over larger spatial scales [50], with a dominance of diatoms over other primary producers expected, as seen in fjord environments with high Si to nitrate ratios [5].

Clearly there are limitations to using such box models and analogue field sites in reconstructing changes in glacial–interglacial Si budgets. The new δ^{30}Si$_{DSi}$ data presented in this review highlights the variation in δ^{30}Si$_{DSi}$ composition of glacial meltwaters. While all glacial systems export isotopically light Si compared with the global average, the variations in composition do not follow simple trends with parameters such as catchment size. Future modelling efforts should attempt to incorporate the variability in δ^{30}Si$_{DSi}$ and δ^{30}Si$_{ASi}$ of ice sheet discharge, as well as the fate of ASi in marine waters, which may require further investigation into the temporal changes in Si isotopic composition of glacial meltwaters.

Nevertheless, the modelling study by Hawkings *et al.* [50] highlights the importance of improving our understanding of glacial fluxes and their role in wider biogeochemical cycles. Improving our knowledge of past climatic events will also enable us to model possible future scenarios more robustly, especially considering the increasing role that the glaciers and ice sheets will have upon these biogeochemical cycles under future warming scenarios.

5. Summary and suggestions for future progress

Our knowledge of glacial environments, particularly subglacial systems, has increased significantly over the past 20 years, enabling greater insight into the hydrology of glaciers and ice sheets and how they may influence global biogeochemical cycles. At a time when glacial meltwater fluxes are expected to increase as a result of global climatic change [26,136,137], it is extremely important that we understand the chemical and physical processes occurring, so that we can make robust predictions of downstream biogeochemical response, including biological production in the future.

The role of glaciers and ice sheets in nutrient cycling, while much debated for the global scale, is likely to be regionally significant, and fluxes are likely to increase as ice mass loss accelerates. Glacial environments may impact regional Si cycles through fluxes of DSi and dissolvable ASi. However, the subglacial processes that are driving the formation of these silica phases need to be better understood and constrained. There are outstanding uncertainties that require attention in the future to ensure we develop a greater understanding of how glacial environments impact Si cycling, in terms of both Si fluxes and δ^{30}Si composition. We therefore propose that, as a community, we should address the following issues.

1. Ensure consistency between sampling methods in glacial environments, especially considering the potential issues from fine-grained glacial flour, colloids and nanoparticulates. A standard protocol for sampling in glacial environments, particularly

to measure isotope compositions, would be beneficial to ensure data can be compared between studies and a glacial database be created.

2. Continue to characterize the δ^{30}Si composition of glacial meltwaters, with an emphasis on capturing longer term temporal variation, so that the drivers of the isotopically light signals can be identified.

3. Continue to improve understanding of subglacial weathering processes, with particular focus on determining the mechanism of ASi formation in glacial environments. This may involve further field measurements, but also the use of novel analytical techniques and laboratory experiments to further understand the subglacial processes driving Si export.

4. Ensure data collected and used in making wider conclusions are representative of a wider range of glacial environments. For example, we are currently lacking studies of Antarctic glaciers in terms of δ^{30}Si composition. Also, Si data are currently much more widely available from west Greenland, compared with east Greenland, where the bedrock lithology is vastly different. More data from smaller alpine glaciers should also be considered important, for example Si fluxes and δ^{30}Si composition of rapidly melting Himalayan and Patagonian glaciers are currently lacking but may have an important role in wider biogeochemical cycles, especially considering their increased vulnerability to present-day climate warming.

5. Determine recycling of glacial nutrients in fjord systems and the implications of this for open ocean export. This will require a combination of field measurements (from the surface to the benthic environment) and modelling experiments to understand the complex nature of fjord environments.

6. Ensure glacial Si concentrations and δ^{30}Si composition are included in the global Si cycle when considering riverine fluxes and that these are applied to biogeochemical models, once we have constrained fluxes and δ^{30}Si composition well enough to be confident of the potential errors of modelling studies.

References

1. Hawkings JR et al. 2015 The effect of warming climate on nutrient and solute export from the Greenland Ice Sheet. *Geochem. Perspect. Lett.* **1**, 94–104. (doi:10.7185/geochemlet.1510)

2. Hawkings JR, Wadham JL, Benning LG, Hendry KR, Tranter M, Tedstone A, Nienow P, Raiswell R. 2017 Ice sheets as a missing source of silica to the polar oceans. *Nat. Commun.* **8**, 14198. (doi:10.1038/ncomms14198)

3. Hawkings JR et al. 2014 Ice sheets as a significant source of highly reactive nanoparticulate iron to the oceans. *Nat. Commun.* **5**, 3929. (doi:10.1038/ncomms4929)

4. Lawson EC *et al.* 2014 Greenland Ice Sheet exports labile organic carbon to the Arctic oceans. *Biogeosciences* **11**, 4015–4028. (doi:10.5194/bg-11-4015-2014)

5. Meire L *et al.* 2016 High export of dissolved silica from the Greenland Ice Sheet. *Geophys. Res. Lett.* **43**, 9173–9182. (doi:10.1002/2016GL070191)

6. Arrigo KR, Dijken GL, Castelao RM, Luo H, Rennermalm ÅK, Tedesco M, Mote TL, Oliver H, Yager PL. 2017 Melting glaciers stimulate large summer phytoplankton blooms in southwest Greenland waters. *Geophys. Res. Lett.* **44**, 6278–6285. (doi:10.1002/2017GL073583)

7. Graly JA, Humphrey NF, Landowski CM, Harper JT. 2014 Chemical weathering under the Greenland Ice Sheet. *Geology* **42**, 551–554. (doi:10.1130/G35370.1)

8. Graly J, Harrington J, Humphrey N. 2017 Combined diurnal variations of discharge and hydrochemistry of the Isunnguata Sermia outlet, Greenland Ice Sheet. *Cryosphere* **11**, 1131–1140. (doi:10.5194/tc-11-1131-2017)

9. Stevenson EI, Fantle MS, Das SB, Williams HM, Aciego SM. 2017 The iron isotopic composition of subglacial streams draining the Greenland ice sheet. *Geochim. Cosmochim. Acta* **213**, 237–254. (doi:10.1016/j.gca.2017.06.002)

10. Bhatia MP, Kujawinski EB, Das SB, Breier CF, Henderson PB, Charette MA. 2013 Greenland meltwater as a significant and potentially bioavailable source of iron to the ocean. *Nat. Geosci.* **6**, 274. (doi:10.1038/ngeo1746)

11. Bhatia MP, Das SB, Xu L, Charette MA, Wadham JL, Kujawinski EB. 2013 Organic carbon export from the Greenland ice sheet. *Geochim. Cosmochim. Acta* **109**, 329–344. (doi:10.1016/j.gca.2013.02.006)

12. Lawson EC, Bhatia MP, Wadham JL, Kujawinski EB. 2014 Continuous summer export of nitrogen-rich organic matter from the Greenland Ice Sheet inferred by ultrahigh resolution mass spectrometry. *Environ. Sci. Technol.* **48**, 14 248–14 257. (doi:10.1021/es501732h)

13. Meire L, Mortensen J, Meire P, Juul-Pedersen T, Sejr MK, Rysgaard S, Nygaard R, Huybrechts P, Meysman FJR. 2017 Marine-terminating glaciers sustain high productivity in Greenland fjords. *Glob. Change Biol.* **23**, 5344–5357. (doi:10.1111/gcb.13801)

14. Tréguer P, Pondaven P. 2000 Silica control of carbon dioxide. *Nature* **406**, 358. (doi:10.1038/35019236)

15. Tréguer P *et al.* 2018 Influence of diatom diversity on the ocean biological carbon pump. *Nat. Geosci.* **11**, 27–37. (doi:10.1038/s41561-017-0028-x)

16. Harrison KG. 2000 Role of increased marine silica input on paleo-pCO$_2$ levels. *Paleoceanography* **15**, 292–298. (doi:10.1029/1999PA000427)

17. Frings PJ, Clymans W, Fontorbe G, De La Rocha CL, Conley DJ. 2016 The continental Si cycle and its impact on the ocean Si isotope budget. *Chem. Geol.* **425**, 12–36. (doi:10.1016/j.chemgeo.2016.01.020)

18. Sutton JN *et al.* 2018 A review of the stable isotope bio-geochemistry of the global silicon cycle and its associated trace elements. *Front. Earth Sci.* **5**, 112. (doi:10.3389/feart.2017.00112)

19. Tréguer PJ, Rocha CLDL. 2013 The world ocean silica cycle. *Annu. Rev. Mar. Sci.* **5**, 477–501. (doi:10.1146/annurev-marine-121211-172346)

20. Opfergelt S, Delmelle P. 2012 Silicon isotopes and continental weathering processes: assessing controls on Si transfer to the ocean. *C. R. Geosci.* **344**, 723–738. (doi:10.1016/j.crte.2012.09.006)

21. Struyf E, Smis A, Van Damme S, Meire P, Conley DJ. 2009 The global biogeochemical silicon cycle. *Silicon* **1**, 207–213. (doi:10.1007/s12633-010-9035-x)

22. McKeague JA, Cline MG. 1963 Silica in soil solutions I. The form and concentration of dissolved silica in aqueous extracts of some soils. *Can. J. Soil Sci.* **43**, 70–82. (doi:10.4141/cjss63-010)

23. White AF. 1995 Chemical weathering rates of silicate minerals in soils. *Rev. Mineral. Geochem.* **31**, 407–461.

24. Cornelis JT, Delvaux B, Georg RB, Lucas Y, Ranger J, Opfergelt S. 2011 Tracing the origin of dissolved silicon transferred from various soil-plant systems towards rivers: a review. *Biogeosciences* **8**, 89–112. (doi:10.5194/bg-8-89-2011)

25. Fettweis X, Hanna E, Lang C, Belleflamme A, Erpicum M, Gallée H. 2013 Important role of the mid-tropospheric atmospheric circulation in the recent surface melt increase over the Greenland ice sheet. *Cryosphere* **7**, 241–248. (doi:10.5194/tc-7-241-2013)

26. Bamber J, den Broeke M, Ettema J, Lenaerts J, Rignot E. 2012 Recent large increases in freshwater fluxes from Greenland into the North Atlantic. *Geophys. Res. Lett.* **39**, L19501. (doi:10.1029/2012GL052552)

27. Tedesco M, Fettweis X, Mote T, Wahr J, Alexander P, Box JE, Wouters B. 2013 Evidence and analysis of 2012 Greenland records from spaceborne observations, a regional climate model and reanalysis data. *Cryosphere* **7**, 615–630. (doi:10.5194/tc-7-615-2013)

28. Fettweis X, Franco B, Tedesco M, van Angelen JH, Lenaerts JTM, van den Broeke MR, Gallée H. 2013 Estimating the Greenland ice sheet surface mass balance contribution to future sea level rise using the regional atmospheric climate model MAR. *Cryosphere* **7**, 469–489. (doi:10.5194/tc-7-469-2013)

29. Trusel LD, Das SB, Osman MB, Evans MJ, Smith BE, Fettweis X, McConnell JR, Noël BPY, van den Broeke MR. 2018 Nonlinear rise in Greenland runoff in response to post-industrial Arctic warming. *Nature* **564**, 104–108. (doi:10.1038/s41586-018-0752-4)

30. Gíslason SR, Snorrason A, Ingvarsson GB, Sigfússon B, Eiríksdóttir ES, Elefsen SO, Hardardottir J, Thorlaksdottir SB, Torssander P. 2006 *Chemical composition, discharge and suspended load in rivers in North-Western Iceland. Report RH-07-2006. Database of the Science Institute and the Hydrological Service of the National Energy Authority*. See https://notendur.hi.is/sigrg/pdfskyrslur/RH-07-2006.pdf.

31. Anderson SP. 2007 Biogeochemistry of glacial landscape systems. *Annu. Rev. Earth Planet. Sci.* **35**, 375–399. (doi:10.1146/annurev.earth.35.031306.140033)

32. Walling DE, Fang D. 2003 Recent trends in the suspended sediment loads of the world's rivers. *Glob. Planet. Change* **39**, 111–126. (doi:10.1016/S0921-8181(03)00020-1)

33. Bartholomew I, Nienow P, Mair D, Hubbard A, King MA, Sole A. 2010 Seasonal evolution of subglacial drainage and acceleration in a Greenland outlet glacier. *Nat. Geosci.* **3**, 408. (doi:10.1038/ngeo863)

34. Tedstone AJ, Nienow PW, Gourmelen N, Dehecq A, Goldberg D, Hanna E. 2015 Decadal slowdown of a land-terminating sector of the Greenland Ice Sheet despite warming. *Nature* **526**, 692. (doi:10.1038/nature15722)

35. Faure F, Mensing TM. 2005 *Isotopes: principles and applications*. Hoboken, NJ: Wiley and Sons.

36. Young ED, Galy A, Nagahara H. 2002 Kinetic and equilibrium mass-dependent isotope fractionation laws in nature and their geochemical and cosmochemical significance. *Geochim. Cosmochim. Acta* **66**, 1095–1104. (doi:10.1016/S0016-7037(01)00832-8)

37. De La Rocha CL, Brzezinski MA, DeNiro MJ. 2000 A first look at the distribution of the stable isotopes of silicon in natural waters. *Geochim. Cosmochim. Acta* **64**, 2467–2477. (doi:10.1016/S0016-7037(00)00373-2)

38. Pogge von Strandmann PAE, Opfergelt S, Lai Y-J, Sigfússon B, Gislason SR, Burton KW. 2012 Lithium, magnesium and silicon isotope behaviour accompanying weathering in a basaltic soil and pore water profile in Iceland. *Earth Planet. Sci. Lett.* **339–340**, 11–23. (doi:10.1016/j.epsl.2012.05.035)

39. De la Rocha CL, Brzezinski MA, DeNiro MJ. 1997 Fractionation of silicon isotopes by marine diatoms during biogenic silica formation. *Geochim. Cosmochim. Acta* **61**, 5051–5056. (doi:10.1016/S0016-7037(97)00300-1)

40. Opfergelt S, Cardinal D, Henriet C, Draye X, André L, Delvaux B. 2006 Silicon isotopic fractionation by banana (Musa spp.) grown in a continuous nutrient flow device. *Plant Soil* **285**, 333–345. (doi:10.1007/s11104-006-9019-1)

41. Geilert S, Vroon PZ, Roerdink DL, Van Cappellen P, van Bergen MJ. 2014 Silicon isotope fractionation during abiotic silica precipitation at low temperatures: inferences from flow-through experiments. *Geochim. Cosmochim. Acta* **142**, 95–114. (doi:10.1016/j.gca.2014.07.003)

42. Oelze M, von Blanckenburg F, Bouchez J, Hoellen D, Dietzel M. 2015 The effect of Al on Si isotope fractionation investigated by silica precipitation experiments. *Chem. Geol.* **397**, 94–105. (doi:10.1016/j.chemgeo.2015.01.002)

43. Georg RB, Reynolds BC, Frank M, Halliday AN. 2006 Mechanisms controlling the silicon isotopic compositions of river waters. *Earth Planet. Sci. Lett.* **249**, 290–306. (doi:10.1016/j.epsl.2006.07.006)

44. Opfergelt S, Burton KW, Pogge von Strandmann PAE, Gislason SR, Halliday AN. 2013 Riverine silicon isotope variations in glaciated basaltic terrains: implications for the Si delivery to the ocean over glacial–interglacial intervals. *Earth Planet. Sci. Lett.* **369–370**, 211–219. (doi:10.1016/j.epsl.2013.03.025)

45. Hughes HJ, Sondag F, Cocquyt C, Laraque A, Pandi A, André L, Cardinal D. 2011 Effect of seasonal biogenic silica variations on dissolved silicon fluxes and isotopic signatures in the Congo River. *Limnol. Oceanogr.* **56**, 551–561. (doi:10.4319/lo.2011.56.2.0551)

46. Cardinal D, Gaillardet J, Hughes HJ, Opfergelt S, André L. 2010 Contrasting silicon isotope signatures in rivers from the Congo Basin and the specific behaviour of organic-rich waters. *Geophys. Res. Lett.* **37**, L12403. (doi:10.1029/2010GL043413)

47. Savage PS, Georg RB, Williams HM, Halliday AN. 2013 Silicon isotopes in granulite xenoliths: insights into isotopic fractionation during igneous processes and the composition of the deep continental crust. *Earth Planet. Sci. Lett.* **365**, 221–231. (doi:10.1016/j.epsl.2013.01.019)

48. Douthitt CB. 1982 The geochemistry of the stable isotopes of silicon. *Geochim. Cosmochim. Acta* **46**, 1449–1458. (doi:10.1016/0016-7037(82)90278-2)

49. Georg RB, Reynolds BC, West AJ, Burton KW, Halliday AN. 2007 Silicon isotope variations accompanying basalt weathering in Iceland. *Earth Planet. Sci. Lett.* **261**, 476–490. (doi:10.1016/j.epsl.2007.07.004)

50. Hawkings JR *et al.* 2018 The silicon cycle impacted by past ice sheets. *Nat. Commun.* **9**, 3210. (doi:10.1038/s41467-018-05689-1)

51. Anderson SP, Drever JI, Frost CD, Holden P. 2000 Chemical weathering in the foreland of a retreating glacier. *Geochim. Cosmochim. Acta* **64**, 1173–1189. (doi:10.1016/S0016-7037(99)00358-0)

52. Anderson SP, Drever JI, Humphrey NF. 1997 Chemical weathering in glacial environments. *Geology* **25**, 399–402. (doi:10.1130/0091-7613(1997)025<0399:CWIGE>2.3.CO;2)

53. Hosein R, Arn K, Steinmann P, Adatte T, Föllmi KB. 2004 Carbonate and silicate weathering in two presently glaciated, crystalline catchments in the Swiss Alps. *Geochim. Cosmochim. Acta* **68**, 1021–1033. (doi:10.1016/S0016-7037(03)00445-9)

54. Torres MA, Moosdorf N, Hartmann J, Adkins JF, West AJ. 2017 Glacial weathering, sulfide oxidation, and global carbon cycle feedbacks. *Proc. Natl Acad. Sci. USA* **114**, 8716–8721. (doi:10.1073/pnas.1702953114)

55. Graly JA, Humphrey NF, Licht KJ. 2018 Two metrics describing the causes of seasonal and spatial changes in subglacial aqueous chemistry. *Front. Earth Sci.* **6**, 195. (doi:10.3389/feart.2018.00195)

56. Wadham JL, Tranter M, Skidmore M, Hodson AJ, Priscu J, Lyons WB, Sharp M, Wynn P, Jackson M. 2010 Biogeochemical weathering under ice: size matters. *Global Biogeochem. Cycles* **24**, GB3025. (doi:10.1029/2009GB003688)

57. Tranter M, Sharp MJ, Lamb HR, Brown GH, Hubbard BP, Willis IC. 2002 Geochemical weathering at the bed of Haut Glacier d'Arolla, Switzerland—a new model. *Hydrol. Process.* **16**, 959–993. (doi:10.1002/hyp.309)

58. Hatton JE, Hendry KR, Hawkings JR, Wadham JL, Kohler TJ, Stibal M, Beaton AD, Bagshaw EA, Telling J. 2019 Investigation of subglacial weathering under the Greenland Ice Sheet using silicon isotopes. *Geochim. Cosmochim. Acta* **247**, 191–206. (doi:10.1016/j.gca.2018.12.033)

59. Chandler DM *et al.* 2013 Evolution of the subglacial drainage system beneath the Greenland Ice Sheet revealed by tracers. *Nat. Geosci.* **6**, 195–198. (doi:10.1038/ngeo1737)

60. Fountain AG, Walder JS. 1998 Water flow through temperate glaciers. *Rev. Geophys.* **36**, 299–328. (doi:10.1029/97RG03579)

61. Anderson SP, Longacre SA, Kraal ER. 2003 Patterns of water chemistry and discharge in the glacier-fed Kennicott River, Alaska: evidence for subglacial water storage cycles. *Chem. Geol.* **202**, 297–312. (doi:10.1016/j.chemgeo.2003.01.001)

62. Bartholomew I, Nienow P, Sole A, Mair D, Cowton T, Palmer S, Wadham J. 2011 Supraglacial forcing of subglacial drainage in the ablation zone of the Greenland ice sheet. *Geophys. Res. Lett.* **38**, L08502. (doi:10.1029/2011GL047063)

63. Hodgkins R. 2001 Seasonal evolution of meltwater generation, storage and discharge at a non-temperate glacier in Svalbard. *Hydrol. Process.* **15**, 441–460. (doi:10.1002/hyp.160)

64. Sharp M, Tranter M, Brown GH, Skidmore M. 1995 Rates of chemical denudation and CO_2 drawdown in a glacier-covered alpine catchment. *Geology* **23**, 61–64. (doi:10.1130/0091-7613(1995)023<0061:ROCDAC>2.3.CO;2)

65. Gibbs MT, Kump LR. 1994 Global chemical erosion during the Last Glacial Maximum and the present: sensitivity to changes in lithology and hydrology. *Paleoceanography* **9**, 529–543. (doi:10.1029/94PA01009)

66. Dubnick A, Kazemi S, Sharp M, Wadham J, Hawkings J, Beaton A, Lanoil B. 2017 Hydrological controls on glacially exported microbial assemblages. *J. Geophys. Res. Biogeosci.* **122**, 1049–1061. (doi:10.1002/2016JG003685)

67. Hindshaw RS, Rickli J, Leuthold J, Wadham J, Bourdon B. 2014 Identifying weathering sources and processes in an outlet glacier of the Greenland Ice Sheet using Ca and Sr isotope ratios. *Geochim. Cosmochim. Acta* **145**, 50–71. (doi:10.1016/j.gca.2014.09.016)

68. Macdonald ML, Wadham JL, Telling J, Skidmore ML. 2018 Glacial erosion liberates lithologic energy sources for microbes and acidity for chemical weathering beneath glaciers and ice sheets. *Front. Earth Sci.* **6**, 212. (doi:10.3389/feart.2018.00212)

69. Montross SN, Skidmore M, Tranter M, Kivimäki A-L, Parkes RJ. 2013 A microbial driver of chemical weathering in glaciated systems. *Geology* **41**, 215–218. (doi:10.1130/G33572.1)

70. Skidmore M, Anderson SP, Sharp M, Foght J, Lanoil BD. 2005 Comparison of microbial community compositions of two subglacial environments reveals a possible role for microbes in chemical weathering processes. *Appl. Environ. Microbiol.* **71**, 6986–6997. (doi:10.1128/AEM.71.11.6986-6997.2005)

71. Žárský JD, Kohler TJ, Yde JC, Falteisek L, Lamarche-Gagnon G, Hawkings JR, Hatton JE, Stibal M. 2018 Prokaryotic assemblages in suspended and subglacial sediments within a glacierized catchment on Qeqertarsuaq (Disko Island), west Greenland. *FEMS Microbiol. Ecol.* **94**, fiy100.

72. Lamarche-Gagnon G *et al.* 2019 Greenland melt drives continuous export of methane from the ice-sheet bed. *Nature* **565**, 73–77. (doi:10.1038/s41586-018-0800-0)

73. Roubeix V, Becquevort S, Lancelot C. 2008 Influence of bacteria and salinity on diatom biogenic silica dissolution in estuarine systems. *Biogeochemistry* **88**, 47–62. (doi:10.1007/s10533-008-9193-8)

74. Stevenson EI, Aciego SM, Chutcharavan P, Parkinson IJ, Burton KW, Blakowski MA, Arendt CA. 2016 Insights into combined radiogenic and stable strontium isotopes as tracers for weathering processes in subglacial environments. *Chem. Geol.* **429**, 33–43. (doi:10.1016/j.chemgeo.2016.03.008)

75. Graly JA, Drever JI, Humphrey NF. 2017 Calculating the balance between atmospheric CO_2 drawdown and organic carbon oxidation in subglacial hydrochemical systems. *Global Biogeochem. Cycles* **31**, 709–727. (doi:10.1002/2016GB005425)

76. Ziegler K, Chadwick OA, Brzezinski MA, Kelly EF. 2005 Natural variations of δ^{30} Si ratios during progressive basalt weathering, Hawaiian Islands. *Geochim. Cosmochim. Acta* **69**, 4597–4610. (doi:10.1016/j.gca.2005.05.008)

77. Blackburn T, Siman-Tov S, Coble MA, Stock GM, Brodsky EE, Hallet B. 2019 Composition and formation age of amorphous silica coating glacially polished surfaces. *Geology* **47**, 347–350. (doi:10.1130/G45737.1)

78. Overeem I, Hudson BD, Syvitski JPM, Mikkelsen AB, Hasholt B, van den Broeke MR, Noël BPY, Morlighem M. 2017 Substantial export of suspended sediment to the global oceans from glacial erosion in Greenland. *Nat. Geosci.* **10**, 859. (doi:10.1038/ngeo3046)

79. Gerringa LJA, Alderkamp A-C, Laan P, Thuróczy C-E, De Baar HJW, Mills MM, van Dijken GL, Haren HV, Arrigo KR. 2012 Iron from melting glaciers fuels the phytoplankton blooms in Amundsen Sea (Southern Ocean): iron biogeochemistry. *Deep Sea Res. Part II Top. Stud. Oceanogr.* **71–76**, 16–31. (doi:10.1016/j.dsr2.2012.03.007)

80. Yde JC, Knudsen NT, Hasholt B, Mikkelsen AB. 2014 Meltwater chemistry and solute export from a Greenland Ice Sheet catchment, Watson River, West Greenland. *J. Hydrol.* **519**, 2165–2179. (doi:10.1016/j.jhydrol.2014.10.018)

81. Telling J *et al.* 2015 Rock comminution as a source of hydrogen for subglacial ecosystems. *Nat. Geosci.* **8**, 851. (doi:10.1038/ngeo2533)

82. Sharp M, Brown GH, Tranter M, Willis IC, Hubbard B. 2017 Comments on the use of chemically based mixing models in glacier hydrology. *J. Glaciol.* **41**, 241–246. (doi:10.1017/S0022143000016142)

83. Tranter M, Raiswell R. 2017 The composition of the englacial and subglacial component in bulk meltwaters draining the Gornergletscher, Switzerland. *J. Glaciol.* **37**, 59–66. (doi:10.1017/S0022143000042805)

84. Sharp M, Tranter M. 2017 Glacier biogeochemistry. *Geochem. Perspect.* **6**, 173–174. (doi:10.7185/geochempersp.6.2)

85. Loucaide S, Van Cappellen P, Behrends T. 2008 Dissolution of biogenic silica from land to ocean: role of salinity and pH. *Limnol. Oceanogr.* **53**, 1614–1621. (doi:10.4319/lo.2008.53.4.1614)

86. Cowton T, Nienow P, Bartholomew I, Sole A, Mair D. 2012 Rapid erosion beneath the Greenland ice sheet. *Geology* **40**, 343–346. (doi:10.1130/G32687.1)

87. Georg RB, Reynolds BC, Frank M, Halliday AN. 2006 New sample preparation techniques for the determination of Si isotopic compositions using MC-ICPMS. *Chem. Geol.* **235**, 95–104. (doi:10.1016/j.chemgeo.2006.06.006)

88. Ding T, Wan D, Wang C, Zhang F. 2004 Silicon isotope compositions of dissolved silicon and suspended matter in the Yangtze River, China. *Geochim. Cosmochim. Acta* **68**, 205–216. (doi:10.1016/S0016-7037(03)00264-3)

89. Ding TP, Gao JF, Tian SH, Wang HB, Li M. 2011 Silicon isotopic composition of dissolved silicon and suspended particulate matter in the Yellow River, China, with implications for the global silicon cycle. *Geochim. Cosmochim. Acta* **75**, 6672–6689. (doi:10.1016/j.gca.2011.07.040)

90. Hughes HJ, Sondag F, Santos RV, André L, Cardinal D. 2013 The riverine silicon isotope composition of the Amazon Basin. *Geochim. Cosmochim. Acta* **121**, 637–651. (doi:10.1016/j.gca.2013.07.040)

91. Morrison MA, Benoit G. 2001 Filtration artifacts caused by overloading membrane filters. *Environ. Sci. Technol.* **35**, 3774–3779. (doi:10.1021/es010670k)

92. Shiller AM. 2003 Syringe filtration methods for examining dissolved and colloidal trace element distributions in remote field locations. *Environ. Sci. Technol.* **37**, 3953–3957. (doi:10.1021/es0341182)

93. Ragueneau O, Savoye N, Del Amo Y, Cotten J, Tardiveau B, Leynaert A. 2005 A new method for the measurement of biogenic silica in suspended matter of coastal waters: using Si:Al ratios to correct for the mineral interference. *Cont. Shelf Res.* **25**, 697–710. (doi:10.1016/j.csr.2004.09.017)

94. Hughes HJ, Delvigne C, Korntheuer M, de Jong J, André L, Cardinal D. 2011 Controlling the mass bias introduced by anionic and organic matrices in silicon isotopic measurements by MC-ICP-MS. *J. Anal. At. Spectrom.* **26**, 1892. (doi:10.1039/c1ja10110b)

95. Crompton JW, Flowers GE, Kirste D, Hagedorn B, Sharp MJ. 2015 Clay mineral precipitation and low silica in glacier meltwaters explored through reaction-path modelling. *J. Glaciol.* **61**, 1061–1078. (doi:10.3189/2015JoG15J051)

96. Wimpenny J, James RH, Burton KW, Gannoun A, Mokadem F, Gíslason SR. 2010 Glacial effects on weathering processes: new insights from the elemental and lithium isotopic composition of West Greenland rivers. *Earth Planet. Sci. Lett.* **290**, 427–437. (doi:10.1016/j.epsl.2009.12.042)

97. Sun X *et al.* 2018 Stable silicon isotopic compositions of the Lena River and its tributaries: implications for silicon delivery to the Arctic Ocean. *Geochim. Cosmochim. Acta* **241**, 120–133. (doi:10.1016/j.gca.2018.08.044)

98. Cornelis J-T, Weis D, Lavkulich L, Vermeire M-L, Delvaux B, Barling J. 2014 Silicon isotopes record dissolution and re-precipitation of pedogenic clay minerals in a podzolic soil chronosequence. *Geoderma* **235–236**, 19–29. (doi:10.1016/j.geoderma.2014.06.023)

99. Panizzo VN, Swann GEA, Mackay AW, Vologina E, Alleman L, André L, Pashley VH, Horstwood MSA. 2017 Constraining modern-day silicon cycling in Lake Baikal. *Global Biogeochem. Cycles* **31**, 556–574. (doi:10.1002/2016GB005518)

100. Hughes HJ, Bouillon S, André L, Cardinal D. 2012 The effects of weathering variability and anthropogenic pressures upon silicon cycling in an intertropical watershed (Tana River, Kenya). *Chem. Geol.* **308–309**, 18–25. (doi:10.1016/j.chemgeo.2012.03.016)

101. Frings PJ, Clymans W, Fontorbe G, Gray W, Chakrapani GJ, Conley DJ, De La Rocha C. 2015 Silicate weathering in the Ganges alluvial plain. *Earth Planet. Sci. Lett.* **427**, 136–148. (doi:10.1016/j.epsl.2015.06.049)

102. Pokrovsky OS, Reynolds BC, Prokushkin AS, Schott J, Viers J. 2013 Silicon isotope variations in Central Siberian rivers during basalt weathering in permafrost-dominated larch forests. *Chem. Geol.* **355**, 103–116. (doi:10.1016/j.chemgeo.2013.07.016)

103. Fontorbe G, De La Rocha CL, Chapman HJ, Bickle MJ. 2013 The silicon isotopic composition of the Ganges and its tributaries. *Earth Planet. Sci. Lett.* **381**, 21–30. (doi:10.1016/j.epsl.2013.08.026)

104. Cockerton HE, Street-Perrott FA, Leng MJ, Barker PA, Horstwood MSA, Pashley V. 2013 Stable-isotope (H, O, and Si) evidence for seasonal variations in hydrology and Si cycling from modern waters in the Nile Basin: implications for interpreting the Quaternary record. *Quat. Sci. Rev.* **66**, 4–21. (doi:10.1016/j.quascirev.2012.12.005)

105. Engström E, Rodushkin I, Ingri J, Baxter DC, Ecke F, Österlund H, Öhlander B. 2010 Temporal isotopic variations of dissolved silicon in a pristine boreal river. *Chem. Geol.* **271**, 142–152. (doi:10.1016/j.chemgeo.2010.01.005)

106. Kohler TJ *et al.* 2017 Carbon dating reveals a seasonal progression in the source of particulate organic carbon exported from the Greenland Ice Sheet. *Geophys. Res. Lett.* **44**, 6209–6217. (doi:10.1002/2017GL073219)

107. Savage PS, Armytage RMG, Georg RB, Halliday AN. 2014 High temperature silicon isotope geochemistry. *Lithos* **190**, 500–519. (doi:10.1016/j.lithos.2014.01.003)

108. Savage PS, Georg RB, Armytage RMG, Williams HM, Halliday AN. 2010 Silicon isotope homogeneity in the mantle. *Earth Planet. Sci. Lett.* **295**, 139–146. (doi:10.1016/j.epsl.2010.03.035)

109. Nienow P. 2014 The plumbing of Greenland's ice. *Nature* **514**, 38. (doi:10.1038/514038a)

110. Bendixen M *et al.* 2017 Delta progradation in Greenland driven by increasing glacial mass loss. *Nature* **550**, 101–104. (doi:10.1038/nature23873)

111. Mavromatis V, Rinder T, Prokushkin AS, Pokrovsky OS, Korets MA, Chmeleff J, Oelkers EH. 2016 The effect of permafrost, vegetation, and lithology on Mg and Si isotope composition of the Yenisey River and its tributaries at the end of the spring flood. *Geochim. Cosmochim. Acta* **191**, 32–46. (doi:10.1016/j.gca.2016.07.003)

112. Opfergelt S, Delvaux B, André L, Cardinal D. 2008 Plant silicon isotopic signature might reflect soil weathering degree. *Biogeochemistry* **91**, 163–175. (doi:10.1007/s10533-008-9278-4)

113. Henderson JH, Syers JK, Jackson ML. 1970 Quartz dissolution as influenced by pH and the presence of a disturbed surface layer. *Isr. J. Chem.* **8**, 357–372. (doi:10.1002/ijch.197000042)

114. Lin IJ, Somasundaran P. 1972 Alterations in properties of samples during their preparation by grinding. *Powder Technol.* **6**, 171–179. (doi:10.1016/0032-5910(72)80074-3)

115. Sánchez-Soto PJ, Carmen Jiménez de Haro M, Pérez-Maqueda LA, Varona I, Pérez-Rodríguez JL. 2000 Effects of dry grinding on the structural changes of kaolinite powders. *J. Am. Ceram. Soc.* **83**, 1649–1657. (doi:10.1111/j.1151-2916.2000.tb01444.x)

116. Schofield O *et al.* 2015 Penguin biogeography along the West Antarctic Peninsula: testing the canyon hypothesis with Palmer LTER observations. *Oceanography* **26**, 204–206. (doi:10.5670/oceanog.2013.63)

117. Hopwood MJ, Carroll D, Browning TJ, Meire L, Mortensen J, Krisch S, Achterberg EP. 2018 Non-linear response of summertime marine productivity to increased meltwater discharge around Greenland. *Nat. Commun.* **9**, 3256. (doi:10.1038/s41467-018-05488-8)

118. Juul-Pedersen T, Arendt KE, Mortensen J, Blicher ME, Søgaard DH, Rysgaard S. 2015 Seasonal and interannual phytoplankton production in a sub-Arctic tidewater outlet glacier fjord, SW Greenland. *Mar. Ecol. Prog. Ser.* **524**, 27–38. (doi:10.3354/meps11174)

119. Annett AL, Skiba M, Henley SF, Venables HJ, Meredith MP, Statham PJ, Ganeshram RS. 2015 Comparative roles of upwelling and glacial iron sources in Ryder Bay, coastal western Antarctic Peninsula. *Mar. Chem.* **176**, 21–33. (doi:10.1016/j.marchem.2015.06.017)

120. Lund-Hansen LC, Hawes I, Holtegaard Nielsen M, Dahllöf I, Sorrell BK. 2018 Summer meltwater and spring sea ice primary production, light climate and nutrients in an Arctic estuary, Kangerlussuaq, west Greenland. *Arct. Antarct. Alp. Res.* **50**, S100025. (doi:10.1080/15230430.2017.1414468)

121. Henley SF, Tuerena RE, Annett AL, Fallick AE, Meredith MP, Venables HJ, Clarke A, Ganeshram RS. 2017 Macronutrient supply, uptake and recycling in the coastal ocean of the west Antarctic Peninsula. *Deep Sea Res. Part II Top. Stud. Oceanogr.* **139**, 58–76. (doi:10.1016/j.dsr2.2016.10.003)

122. Sherrell RM, Annett AL, Fitzsimmons JN, Roccanova VJ, Meredith MP. 2018 A 'shallow bathtub ring' of local sedimentary iron input maintains the Palmer Deep biological hotspot on the West Antarctic Peninsula shelf. *Phil. Trans. R. Soc. A* **376**, 20170171. (doi:10.1098/rsta.2017.0171)

123. Wehrmann LM, Formolo MJ, Owens JD, Raiswell R, Ferdelman TG, Riedinger N, Lyons TW. 2014 Iron and manganese speciation and cycling in glacially influenced high-latitude fjord sediments (West Spitsbergen, Svalbard): evidence for a benthic recycling-transport mechanism. *Geochim. Cosmochim. Acta* **141**, 628–655. (doi:10.1016/j.gca.2014.06.007)

124. Kanna N, Sugiyama S, Ohashi Y, Sakakibara D, Fukamachi Y, Nomura D. 2018 Upwelling of macronutrients and dissolved inorganic carbon by a subglacial freshwater driven plume in Bowdoin Fjord, Northwestern Greenland. *J. Geophys. Res. Biogeosci.* **123**, 1666–1682. (doi:10.1029/2017JG004248)

125. Jeandel C, Oelkers EH. 2015 The influence of terrigenous particulate material dissolution on ocean chemistry and global element cycles. *Chem. Geol.* **395**, 50–66. (doi:10.1016/j.chemgeo.2014.12.001)

126. Hopwood MJ, Connelly DP, Arendt KE, Juul-Pedersen T, Stinchcombe MC, Meire L, Esposito M, Krishna R. 2016 Seasonal changes in Fe along a glaciated Greenlandic fjord. *Front. Earth Sci.* **4**, 15. (doi:10.3389/feart.2016.00015)
127. Sun X, Olofsson M, Andersson PS, Fry B, Legrand C, Humborg C, Mörth C-M. 2014 Effects of growth and dissolution on the fractionation of silicon isotopes by estuarine diatoms. *Geochim. Cosmochim. Acta* **130**, 156–166. (doi:10.1016/j.gca.2014.01.024)
128. Hendry KR *et al.* The biogeochemical impact of glacial meltwater from Southwest Greenland. *Prog. Oceanogr.* **176**, 102126. (doi:10.1016/j.pocean.2019.102126)
129. Frajka-Williams E, Rhines PB. 2010 Physical controls and interannual variability of the Labrador Sea spring phytoplankton bloom in distinct regions. *Deep Sea Res. Part I Oceanogr. Res. Pap.* **57**, 541–552. (doi:10.1016/j.dsr.2010.01.003)
130. Oliver H *et al.* 2018 Exploring the potential impact of Greenland meltwater on stratification, photosynthetically active radiation, and primary production in the Labrador Sea. *J. Geophys. Res. Oceans* **123**, 2570–2591. (doi:10.1002/2018JC013802)
131. Dickson R, Rudels B, Dye S, Karcher M, Meincke J, Yashayaev I. 2007 Current estimates of freshwater flux through Arctic and subarctic seas. *Prog. Oceanogr.* **73**, 210–230. (doi:10.1016/j.pocean.2006.12.003)
132. Myers PG, Donnelly C, Ribergaard MH. 2009 Structure and variability of the West Greenland Current in summer derived from 6 repeat standard sections. *Prog. Oceanogr.* **80**, 93–112. (doi:10.1016/j.pocean.2008.12.003)
133. De La Rocha CL, Brzezinski MA, DeNiro MJ, Shemesh A. 1998 Silicon-isotope composition of diatoms as an indicator of past oceanic change. *Nature* **395**, 680. (doi:10.1038/27174)
134. Beucher CP, Brzezinski MA, Crosta X. 2007 Silicic acid dynamics in the glacial sub-Antarctic: implications for the silicic acid leakage hypothesis. *Global Biogeochem. Cycles* **21**, GB3015. (doi:10.1029/2006GB002746)
135. Froelich PN, Blanc V, Mortlock RA, Chillrud SN. 1992 River fluxes of dissolved silica to the ocean were higher during glacials: Ge/Si in diatoms, rivers, and oceans. *Paleoceanography* **7**, 739–767. (doi:10.1029/92PA02090)
136. Milner AM *et al.* 2017 Glacier shrinkage driving global changes in downstream systems. *Proc. Natl Acad. Sci. USA* **114**, 9770–9778. (doi:10.1073/pnas.1619807114)
137. Bronselaer B, Winton M, Griffies SM, Hurlin WJ, Rodgers KB, Sergienko OV, Stouffer RJ, Russell JL. 2018 Change in future climate due to Antarctic meltwater. *Nature* **564**, 53–58. (doi:10.1038/s41586-018-0712-z)